Soft Matter

PAPER

View Article Online
View Journal



Cite this: DOI: 10.1039/d5sm01024a

# Effect of external salt solution concentration on carboxyl dissociation degree ($\alpha$) and p$K_a$ of weak polyelectrolyte membranes for sustainable technologies

Yongha Kim,[a] Charleen M. Rahman,[a] Michael A. Shaqfeh,[a] Kyle M. Tierney,[a] Andrew J. Lukaszewski,[a] Nikitha S. Kanumuru,[b] Dae Eun Kang[c] and Hee Jeung Oh *[abde]

Understanding the dissociation process of weakly charged polymers under varied external salt conditions is critical to develop innovative charged polymer membranes with desirable transport properties for sustainable technologies. We previously designed a series of weakly charged polymer membranes, *i.e.*, cross-linked acrylic acid (AA)–poly(ethylene glycol) diacrylate (PEGDA) (AA–PEGDA) random copolymer networks with a wide ion-exchange capacity (IEC = 0–4 mequiv. per g) range and limited water swelling. Here, we report the dissociation process in the representative chemical structure of AA–PEGDA series, *i.e.*, 10-2 AA–PEGDA network (PEGDA cross-linker length $n$ = 10, mIEC = 2 mequiv. per g) in different external salt concentration solutions (0–1 M NaCl (aq)). When titrated with a strong base (NaOH), both POT titration (detecting a solution phase) and ATR–FTIR analysis (probing a polymer phase) well describe the dissociation process and yield similar ranges of dissociation parameters ($\alpha$, p$K_a$). The dissociation behavior follows the modified Henderson–Hasselbalch equation, showing lower p$K_a$ values with increasing external salt concentrations. The governing molecular factor for dissociation was determined by comparing four length scales ($r_c$, $r_{ion}$, $l_B$, and $r_D$) in the system, including (1) charged group distance in a polymer ($r_c$), (2) distance between salt ions in an external solution ($r_{ion}$), the respective (3) Bjerrum length ($l_B$) and (4) Debye screening length ($r_D$). At the lower external salt concentration (0 M $\leq C_{NaCl} \leq$ 0.01 M), the relative standing of these length scales ($r_c < l_B \ll r_D < r_{ion}$) indicates that the enhanced electrostatic interaction in dilute conditions suppresses the dissociation in the network and thus increases p$K_a$. At the higher salt concentration (0.1 M $\leq C_{NaCl} \leq$ 1.0 M), the different order of these length scales ($r_D \ll r_c \lesssim l_B \lesssim r_{ion}$) represents that the screened electrostatic interaction *via* the added external salts promotes the dissociation and thus decreases p$K_a$. As the external salt concentration increases (0–1.0 M NaCl), water swelling in the network slightly decreases due to osmotic deswelling. However, the lower water swelling has very little effect on effectively decreasing the charged group distance in the polymer ($r_c$), and thus, leads to little substantive influence on the electrostatic interaction (consequently, the dissociation). Therefore, the screened electrostatic interaction by the added external salts dictates the dissociation and p$K_a$ in our system. Our multiscale analysis of dissociation across varying external salt concentrations provides a pathway to tune the dissociation behavior of weakly charged polymers and achieve desired transport properties for target applications.

Received 7th October 2025,
Accepted 29th April 2026

DOI: 10.1039/d5sm01024a

rsc.li/soft-matter-journal

[a] Department of Chemical Engineering, The Pennsylvania State University, University Park, PA 16802, USA. E-mail: hjoh@psu.edu; Tel: +1 814-863-9085
[b] Department of Materials Science and Engineering, The Pennsylvania State University, University Park, Pennsylvania 16802, USA
[c] Department of Chemistry, The Pennsylvania State University, University Park, Pennsylvania 16802, USA
[d] Institute of Energy and Environment (IEE), The Pennsylvania State University, University Park, Pennsylvania 16802, USA
[e] Advanced Manufacturing and Design, The Pennsylvania State University, University Park, Pennsylvania 16802, USA

## 1. Introduction

Charged polymers can offer selective and controlled transport of small molecules (*e.g.*, water, ion, gas) across the polymers, enabling a broad range of membrane-based applications in energy, environment and health.[1–6] Relevant applications include gas, liquid and vapor separations, energy generation (*e.g.*, batteries, fuel cells), resource recovery, environmental remediation and health-related devices, amongst others.[5–15]

Varied charged group content (type and concentration) combined with polymer architecture and topology provides a useful toolbox in controlling ion and water transport across the polymer membranes. However, it is often challenging to understand the effect of charged group content on ion transport in the polymer membranes due to its coupled effects with polymer morphology and high water swelling.[16–21] For instance, changing charged group concentration in one polymer backbone requires different processing variables (*e.g.*, solvent, formation methods), resulting in different polymer morphologies. Also, increased charged group content leads to high water swelling in the polymers. High water swelling often overshadows the effects originating from charged group contents on ion transport in the polymers. These coupled influences with polymer morphology and high water swelling on ion transport make a systematic comparison difficult. These difficulties hinder our mechanistic understanding of ion transport in the charged polymer membranes.

To overcome the current limitations in literature, we previously designed a series of weak polyelectrolyte membranes, *i.e.*, cross-linked acrylic acid (AA)–poly(ethylene glycol) diacrylate (PEGDA) (AA–PEGDA) random copolymer networks with a wide ion-exchange capacity (IEC = 0–4 mequiv. per g) range and limited water swelling.[22,23] Weakly acidic, acrylic acid (AA) monomer was chosen as a charged block. Poly(ethylene glycol)-diacrylates (PEGDAs) with different molecular weights were used as cross-linkers to control the distance between network junctions and thus limit high water swelling. In this model polymer, using one fixed chemical structure, the charged group concentration can be systematically altered (degree of ionization, $\alpha$ = 0–1) as the external pH is changed between pH = 3–12. If pH $\ll$ p$K_a$, almost all of dissociable charged groups (COOH in this study) do not dissociate (degree of ionization, $\alpha$ = 0) and the polymer behaves like an uncharged polymer. If pH = p$K_a$, one half of the dissociable charged groups (COOH) dissociates to present as carboxylate groups ($COO^-$) and thus, $\alpha$ is 0.5. If pH $\gg$ p$K_a$, all dissociable charged groups (COOH) dissociate ($\alpha$ = 1) and the polymer is fully ionized. Thus, using one fixed chemical structure, we can systematically change the amount of charged groups in the polymer without altering polymer morphology while limiting high water swelling. This model system enables us to develop a systematic, mechanistic understanding of ion and water transport in charged polymer membranes.

Toward this goal, it is essential to understand the dissociation process in weakly charged AA–PEGDA series *vs.* the external pH. Compared to the extensively studied non-polymeric acids and bases in dissociation, dissociation behavior of polyelectrolyte materials and ion-exchange resins is still largely underdeveloped.[24–26] In polyelectrolyte polymers, dissociation parameters such as degree of ionization ($\alpha$) and the negative logarithm of apparent acid dissociation constant (p$K_a$) are dependent on chemical structure, morphology, processing variables (*e.g.*, form factors) and external test conditions. Thus, it is important to use a systematic polymer platform to understand the dissociation process in the polyelectrolyte polymers. In literature, however, many polyelectrolyte polymers including acrylic acid (AA)-containing polymers were studied using different forms (*e.g.*, dissolved polymer solutions, porous beads with different porosities, films, or composite structures), different cross-linker content (*e.g.*, cross-linker type and concentration) and varied test conditions (*e.g.*, salt type and concentration). These differences make a systematic comparison difficult among these reports.[27–30] On the other hand, our AA–PEGDA series in this study was prepared with systematically varied polymer composition (*e.g.*, AA monomer content (the amount of dissociable charged groups) and PEGDA cross-linker content with different cross-linker length, $n$ = 10 and 13) and was formed into thin film membranes of a uniform–thickness. Thus, this AA–PEGDA system enables a systematic study of dissociation process in weakly charged polymers.

In this context, we reported the degree of ionization ($\alpha$) and p$K_a$ of AA–PEGDA series in dilute (DI water) and concentrated salt (1 M NaCl (aq)) solutions *via* two rigorous analytical methods including (1) potentiometric (POT) titration which measures dissociation in a solution phase and (2) ATR–FTIR analysis which detects dissociation in a polymer phase.[23,39] Both methods (probing solution and polymer phases together) faithfully describe the molecular-level physical picture of dissociation process in AA–PEGDA series. As pH increases between pH = 5–12, the degree of ionization ($\alpha$) increases between 0–1, following the modified Henderson–Hasselbalch equation. While our previous reports serve as a baseline to understand the dissociation process as a function of polymer composition (mIEC and PEGDA cross-linker length, $n$) as well as in two representative external salt conditions (dilute (DI water) and concentrated (1 M NaCl (aq)) solutions), in real-life applications, a polymer membrane is frequently used in a broad range of external salt conditions in complex environments. Different external salt concentrations significantly affect dissociation behavior and transport properties in weakly charged polymers.[6,10,31,32] Therefore, it was necessary to systematically study the effect of external salt concentration on the dissociation process using one representative chemical structure of AA–PEGDA series, *i.e.*, 10-2 AA–PEGDA network with PEGDA cross-linker length $n$ = 10 and the maximum ion-exchange capacity (mIEC) of 2 mequiv. per g. The 10-2 network was chosen for this study because its IEC (effective ion-exchange capacity (eIEC) = 0–2 mequiv $g^{-1}$) and water swelling ($\phi_w$ = 0.30–0.54) ranges are relevant to other commercially available and/or widely studied polyelectrolyte membranes.[33–38]

Therefore, we report the dissociation process in the representative 10-2 AA–PEGDA network (mIEC = 2 mequiv. per g and PEGDA cross-linker length $n$ = 10) in varied external salt concentration solutions including 0 M (DI water), 0.01 M, 0.1 M and 1 M NaCl (aq) solutions. The new dissociation data in 0.01 M and 0.1 M NaCl (aq) solutions are compared with the dissociation behavior in 0 M and 1 M NaCl (aq) solutions from our previous studies.[22,23,39] Two analytical methods are used to thoroughly record the dissociation process in both 1) a solution phase (*via* POT titration) and 2) a polymer phase (*via* ATR–FTIR analysis). By systematically changing the external salt concentrations from a 0 M to 1 M NaCl (aq) solution, we record degree

 

of ionization ($\alpha$) *vs.* the external pH as well as p$K_a$ trends. In addition, to understand the dissociation behavior before titration, we report pre-titration dissociation degree ($\alpha$) prior to adding a strong base (NaOH in this study) *vs.* the external salt concentrations. To interpret the dissociation data and determine p$K_a$, we use the modified Henderson–Hasselbalch equation.

Our rigorous interpretation of dissociation data was conducted in three ways. First, to determine the governing molecular variables on the dissociation, we record the dissociation parameter (p$K_a$) with respect to charged group concentration ($C_c^m$), equilibrium water swelling ($\phi_w$) and external salt concentration ($C_s$) in the system. The motivation for introducing charged group concentration ($C_c^m$) and water swelling ($\phi_w$) comes from the fact that, changing external salt concentration ($C_s$) leads to different water swelling ($\phi_w$) due to an osmotic deswelling effect, and thus, different charged group concentration ($C_c^m$) in the polymers. These three linked variables ($C_c^m$, $\phi_w$, $C_s$) need to be understood cooperatively in our system. Secondly, to understand the dominant molecular factors on the electrostatic interaction (thus, dissociation) in our system, we compared four relevant molecular-level length scales, *i.e.*, (1) the charged group distance in a polymer ($r_c$), (2) the distance between salt ions in an external solution ($r_{ion}$), the respective (3) Bjerrum length ($l_B$) and (4) Debye screening length ($r_D$) in the different external salt solutions. The relative order of these four length scales broadly dictates the electrostatic interaction and thus dissociation. Thirdly, we compare the p$K_a$ trend in this study with other AA-containing polymers in the literature. Our goal is to build a comprehensive understanding of dissociation in similar weakly charged polymers. Together, our multiscale analysis of dissociation provides a pathway to tune the dissociation behavior of weakly charged polymers across varying external salt concentrations.

## 2. Materials and experimental

### 2.1. Materials

A series of cross-linked acrylic acid (AA)–poly(ethylene glycol) diacrylate (PEGDA) (AA–PEGDA) random copolymer networks was synthesized *via* UV-induced free radical polymerization as shown in Fig. 1a and b. Acrylic acid (AA, 8.00181, Millipore Sigma, Burlington, MA) was a weakly charged monomer with a carboxylic acid group (COOH). Poly(ethylene glycol) diacrylates (PEGDAs, 437441 and 455008, Millipore Sigma, Burlington, MA) with different molecular weights ($\bar{M}_n$ = 575 g mol$^{-1}$ and $\bar{M}_n$ = 700 g mol$^{-1}$) were used as cross-linkers. Deionized (DI) water (18.2 MΩ cm, Millipore Direct-Q 5 UV system, Merck, Germany) was used as a solvent and 2, 2-dimethoxy-2-phenylacetophenone (DMPA, 196118, Millipore Sigma) was used as a photoinitiator. All reactants were purchased and used as received. Sodium chloride (NaCl, S9888, Millipore Sigma) was used to prepare aqueous salt solutions. Sodium hydroxide (NaOH, S5881, Millipore Sigma) was used for titration.

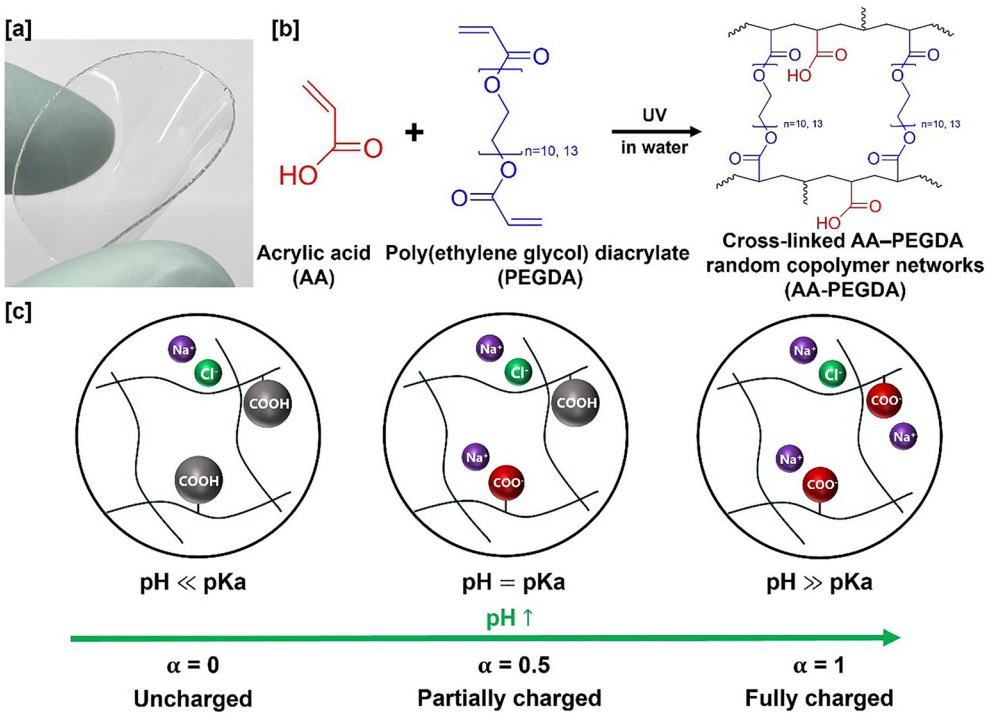


Fig. 1 (a) Transparent free-standing 10-2 AA–PEGDA network film with a uniform thickness. The 10-2 formulation has the maximum ion-exchange capacity (mIEC) = 2 mequiv. per g with PEGDA cross-linker length, $n$ = 10. (b) Chemical structure of cross-linked acrylic acid-poly(ethylene glycol) diacrylate (AA–PEGDA) network *via* UV-induced free radical polymerization. (c) Schematic shows the dissociation process *vs.* pH.

### 2.2. Membrane preparation

Free-standing transparent films of AA–PEGDA networks were prepared with uniform thickness (with a variability <3–5%) (see Fig. 1a).[22,23,39] A homogenous transparent prepolymer mixture was prepared by vigorously stirring a known concentration of AA monomer, PEGDA cross-linker, DI water (solvent), and DMPA (photoinitiator) for 30 m in an aluminum foil-covered glass jar, followed by a gentle 30 m mixing (see Table S1). 3 mL of the prepolymer mixture was poured onto a leveled quartz plate (CGQ-0620-20, Chemglass Life Sciences, Vineland, NJ) where four spacers of 305 μm thickness (19470, Precision Brand, Downers Grove, IL) were placed at the edges. Another quartz plate sandwiched the prepolymer mixture. The assembled quartz plates were UV-cured for 90 s in a Spectrolinker (XL-1000 UV Crosslinker, 254 nm, Spectronics Corporation, Melville, NY) to form a uniform-thickness transparent film. The formed film was then soaked in DI water for 2–3 days where water was replaced frequently to remove unreacted reactants from the network. Circular polymer coupons (diameter is 2.2 cm) were cut using a punch die (66002, Mayhew Steel Products, Turners Falls, MA) for further characterization. The average mass conversion rate of AA–PEGDA series was 98.4 ± 1.2%, supporting successful polymerization, as reported in our previous papers.[22,23]

Nomenclature of AA–PEGDA series in this study is *n*-mIEC where *n* denotes the number of ethylene oxide (EO) repeating unit in a PEGDA cross-linker (*i.e.*, *n* = 10 or 13) and mIEC indicates the maximum ion-exchange capacity of the polymer. For instance, 10-2 AA–PEGDA network contains 10 of EO repeating units between two network junctions and its mIEC is 2 mequiv. per g.

### 2.3. Theoretical cross-linking density ($\nu_t$)

Theoretical cross-linking density ($\nu_t$) of a polymer was determined from the concentration of vinyl (C═C) groups in a PEGDA cross-linker in an AA–PEGDA network as:[40,41]

$$\nu_t\left[\frac{\text{Moles of vinyl groups [mol]}}{\text{Volume of a dry polymer [cm}^3\text{]}}\right] = 2\cdot\frac{m_c/\bar{M}_n}{m_d/\rho_p} \quad (1)$$

where $m_c$ is the mass of a PEGDA cross-linker [g], $m_d$ is the mass of a dry polymer [g], $\bar{M}_n$ is the number-average molecular weight of the PEGDA cross-linker [g mol$^{-1}$], and $\rho_P$ is the polymer density [g cm$^{-3}$]. The prefactor of 2 means that each PEGDA cross-linker contains two vinyl groups for cross-linking.

### 2.4. Potentiometric (POT) titration

Potentiometric (POT) titration was performed to control the degree of dissociation (ionization) ($\alpha$) in AA–PEGDA series. A circular polymer coupon (diameter is 2.2 cm) was dried in a vacuum oven (281A, Thermo Fisher Scientific, Waltham, MA) at 50 °C for 2 days to remove residual water in the polymer. Dry masses ($m_d$) of the polymer coupon were recorded using an analytical balance (MS304TS/00, Mettler Toledo, Columbus, OH) until equilibrium was reached. The dry coupon was then immersed in 100 mL of NaCl (aq) solutions with different NaCl concentrations (*i.e.*, 0 M, 0.01 M, 0.1 M, and 1 M NaCl (aq) solutions) at room temperature (21–22 °C). Note that, prior to experiments, DI water used for titration and salt solution preparation was equilibrated with atmospheric $CO_2$ (g) for 24 h at room temperature to achieve an equilibrium amount of dissolved $CO_2$ in water (see Section 4.1). After equilibrated with $CO_2$ (g) in air, pH in the different NaCl (aq) solutions was in the range of 5.7–6.3 (with a variability <2–3%), as consistent with the reported values (pH ~ 5.65) in literature.[22,23,39,42,43]

Next, a known amount of 0.1 M NaOH solution ($x_{NaOH}$ [mequiv. per g]) was added to control the pH in the external solution (see Table S2). The polymer coupon was titrated on an orbital shaker (Labnique, Hunt Valley, MD) for 1 day to reach equilibrium. Then the pH of the external solution was recorded using a pH meter (SevenDirect SD50, Mettler Toledo, Columbus, OH). The mass of the swollen polymer coupon was also measured until equilibrium was achieved. Subsequently, the swollen polymer coupon was dried in a vacuum oven at 50 °C overnight for further characterization. To confirm the chemical stabilities of the polymer during titration, ATR–FTIR was run at each step. Degree of ionization ($\alpha$) of the polymer coupon was determined by best fitting the data using the modified Henderson–Hasselbalch equation. Detailed procedures are shown in Fig. S2 as reported previously.[22,23,25–28,39,44]

### 2.5. Polymer characterization

**2.5.1. Polymer density ($\rho_P$).** Polymer density ($\rho_P$ [g cm$^{-3}$]) was determined using a density measurement kit (ML-DNY-43, Mettler Toledo, Columbus, OH) *via* the Archimedes' principle as:[45,46]

$$\rho_p = \frac{m_d}{m_d - m_l}\times\rho_l \quad (2)$$

where $m_d$ and $m_l$ are the masses of a dry polymer coupon in air and an auxiliary liquid, respectively, and $\rho_l$ is the density of the auxiliary liquid. In this study, the auxiliary liquid was *n*-heptane (34873, Millipore Sigma, Burlington, MA) since AA–PEGDA series shows negligible uptake of *n*-heptane in the polymers.[22,23,39,47] Polymer density values are shown in Fig. S19.

**2.5.2. Equilibrium water swelling ($\phi_w$).** Equilibrium water swelling ($\phi_w$) of AA–PEGDA series was determined *via* a gravimetric water uptake experiment. A polymer coupon (diameter is 2.2 cm) was dried in a vacuum oven at 50 °C for 2 days and equilibrium dry mass ($m_d$) was recorded. The dry coupon was then immersed in DI water or different NaCl (aq) solutions at ambient temperature before and after titration. After gently removing excess water on the polymer surface using dust–free tissue papers, wet masses ($m_w$) were periodically measured until equilibrium was reached. Equilibrium water uptake [g g$^{-1}$] is expressed as:[33,48,49]

$$w_u\left[\frac{\text{Mass of sorbed water[g]}}{\text{Mass of a dry polymer [g]}}\right] = \frac{m_w - m_d}{m_d} \quad (3)$$

Equilibrium water volume fraction in a swollen polymer ($\phi_w$ [$cm^3$ of sorbed water/$cm^{-3}$ of a swollen polymer]) was determined *via* assuming the volume additivity[33,48,49] of water in a swollen polymer as:

$$\phi_w\left[\frac{\text{Volume of sorbed water in a swollen polymer }[cm^3]}{\text{Volume of a swollen polymer }[cm^3]}\right] = \frac{(m_w - m_d)/\rho_w}{(m_w - m_d)/\rho_w + m_d/\rho_p} \quad (4)$$

where $\rho_w$ and $\rho_P$ are the densities of water (1.0 g $cm^{-3}$) and the dry polymer, respectively.

**2.5.3. ATR–FTIR.** Chemical structure and charged group concentrations (dissociable COOH and dissociated $COO^-$ groups) of AA–PEGDA series were characterized using an attenuated total reflectance Fourier–transform infrared spectroscopy (ATR–FTIR, NICOLET iS50 FTIR, Thermo Fisher Scientific, Waltham, MA). Before titration, a polymer coupon (diameter is 2.2 cm) was soaked in 100 mL of different NaCl (aq) solutions (*i.e.*, 0 M, 0.01 M, 0.1 M, and 1 M NaCl (aq) solutions) for 1–2 days at room temperature. Then the polymer coupon was dried in a vacuum oven overnight at 50 °C for ATR–FTIR analysis. After titration, the polymer coupon was analyzed again using ATR–FTIR. The amounts of dissociable COOH and dissociated $COO^-$ groups were quantified using the method reported previously.[22,23,26,39,50] All spectra were recorded in the range of 500–4000 $cm^{-1}$ with a resolution of 4 $cm^{-1}$ and 64 scans. Background spectra was subtracted to obtain the sample spectra using OMNIC software (Thermo Fisher Scientific, Waltham, MA).

# 3. Theory

## 3.1. Determination of charged group content

Carboxyl acid (COOH) groups in weakly charged AA–PEGDA series dissociate to form carboxylate ($COO^-$) groups as:[24]

$$R\text{–}COOH \leftrightarrows R\text{–}COO^- + H^+ \quad (5)$$

Degree of ionization ($\alpha$) is defined as the ratio between the amount of dissociated carboxylate ($COO^-$) groups [mol] and the amount of total dissociable carboxylic acid (COOH) groups [mol] as:[24]

$$\alpha = \frac{[R - COO^-]}{[R - COOH] + [R - COO^-]} \quad (0 \le \alpha \le 1) \quad (6)$$

In AA–PEGDA series, the maximum ion-exchange capacity (mIEC, mmol equivalent of $H^+$ per grams of a dry polymer [mequiv. per g]) represents the total concentration of *dissociable* charged groups (COOH) in a polymer. Thus, mIEC of the polymer is only affected by the AA monomer content in the polymer.[22–24,39] On the other hand, effective ion-exchange capacity (eIEC) represents the concentration of dissociated charged groups ($COO^-$) under a given condition. Subsequently, eIEC value is dependent on both the AA monomer content in the polymer and the external pH. Therefore, mIEC and eIEC are related by the degree of ionization ($\alpha$) as:

$$\text{eIEC} = \text{mIEC}\cdot\alpha \quad (0 \le \alpha \le 1) \quad (7)$$

Additionally, the amount of dissociated charged ($COO^-$) group in a polymer can be expressed as the charged group concentration in sorbed water of a swollen polymer ($C_c^m$ [mol $L^{-1}$], subscript $_c$ notes charged groups whereas superscript $^m$ means a membrane phase) as:[16,18,51]

$$C_c^m = \frac{\text{Moles of dissociated charged groups in a swollen polymer [mol]}}{\text{Volume of sorbed water in a swollen polymer [L]}} = \frac{\text{eIEC}\cdot\rho_w}{w_u} \quad (8)$$

## 3.2. Degree of ionization ($\alpha$) before titration

Before titration (without adding a strong base), degree of ionization ($\alpha$) of AA–PEGDA series was recorded by measuring the pH change in an external solution equilibrated with a polymer coupon, as reportedly previously[22,23,39] (see Fig. S1). If a small fraction of carboxylic acid (COOH) groups in the polymer coupon dissociates and presents as carboxylate ($COO^-$) groups, $H_3O^+$ concentration in the external solution increases correspondingly. By measuring the increased $H_3O^+$ concentration (pH) in the external solution, the degree of ionization ($\alpha$) of the polymer can be determined as:[22,23,39]

$$\alpha = \frac{\text{Moles of dissociated } H_3O^+ \text{ in a polymer coupon [mol]}}{\text{Moles of total dissociable charged (COOH) groups in a polymer coupon [mol]}} = \frac{V_s \times \left(10^{-\text{pH of a solution after soaking a coupon}} - 10^{-\text{pH of a solution before soaking a coupon}}\right)}{\text{Moles of total dissociable charged (COOH) groups in a polymer coupon [mol]}} \quad (9)$$

where $V_s$ is the volume of the external solution (100 mL). The total number of dissociable charged (COOH) groups was calculated from the chemical composition of AA–PEGDA series (the average mass conversion rate of the formed AA–PEGDA series is 98.4 ± 1.2%[22,23]).

## 3.3. Degree of ionization ($\alpha_{pH}$) *via* POT titration

During POT titration, degree of ionization ($\alpha_{pH}$) of a polymer was determined from the added amount of NaOH ($x_{NaOH}$) (subscript $_{pH}$ notes that the degree of ionization ($\alpha$) was determined by potentiometric pH titration). As a strong base (NaOH) is added, hydroxide anions ($OH^-$) from the NaOH react with released $H^+$ from dissociated carboxylate ($COO^-$) groups, forming water ($H_2O$). With increasing amount of added NaOH, the amount of dissociated $COO^-$ groups increases, respectively. When the added NaOH amount ($x_{NaOH}$) is smaller than the mIEC of the polymer, the corresponding fraction of dissociable COOH groups with respect to the added NaOH amount ($x_{NaOH}$/mIEC) can dissociate. When the amount of added NaOH equals the total amount of dissociable COOH groups of the polymer

($x_{NaOH}$ = mIEC), all COOH groups dissociate and its degree of ionization ($\alpha_{pH}$) becomes 1. Thus, the degree of ionization ($\alpha_{pH}$) can be calculated from the amount of added NaOH as:[22,23,39]

$$\alpha_{pH} \approx \begin{cases} x_{NaOH}/\text{mIEC} & \text{if } x_{NaOH} < \text{mIEC} \\ 1 & \text{if } x_{NaOH} \geq \text{mIEC} \end{cases} \quad (10)$$

### 3.4. Degree of ionization ($\alpha_{IR}$) *via* ATR–FTIR

Degree of ionization ($\alpha_{IR}$) of a polymer was also quantified using ATR–FTIR analysis (subscript $_{IR}$ indicates that the degree of ionization ($\alpha$) was obtained *via* IR analysis). The detailed peak assignments and calculation methods of AA–PEGDA networks have been discussed in our previous reports[22,23,39] and are summarized in Sections S1 and S2. According to the Beer–Lambert law, the degree of ionization ($\alpha_{IR}$) of a polymer can be expressed as:

$$\alpha_{IR} = \frac{A_{COO^-}}{A_{COO^-} + A_{COOH} \bullet F} \quad (11)$$

where $A_{COO^-}$ is the area under the curve at 1575 $cm^{-1}$ (from dissociated $COO^-$ groups), $A_{COOH}$ is the subtracted area under the curve at 1700 $cm^{-1}$ (from dissociable COOH groups), and $F$ is the ratio between $A_{COO^-}$ at the highest pH (pH = 11–12 where all COOH groups dissociate and present as $COO^-$) and $A_{COOH}$ at the lowest pH (pH = 3–6 where almost all COOH groups are not dissociated and present as COOH). Similar methods have been reported by other researchers.[26,50]

### 3.5. p$K_a$ *via* the modified Henderson–Hasselbalch equation

The negative logarithm of apparent acid dissociation constant (p$K_a$) of a polymer is expressed as:[24]

$$pK_a = -\log\frac{[H^+][R{-}COO^-]}{[R{-}COOH]} \quad (12)$$

pH is the negative logarithm of $H_3O^+$ concentration ($[H_3O^+]$) in an external solution as:[24]

$$pH = -\log[H_3O^+] \quad (13)$$

The degree of ionization ($\alpha$), p$K_a$ and pH of a system can be related using the Henderson–Hasselbalch equation as:[24]

$$pH = pK_a + \log(\alpha/(1 - \alpha)) \quad (14)$$

The modified Henderson–Hasselbalch equation can be used to best fit the data as:[25]

$$pH = pK_a + B\log(\alpha/(1 - \alpha)) \quad (15)$$

where $B$ is the fitting parameter. The degrees of ionization, $\alpha_{pH}$ (*via* POT titration) and $\alpha_{IR}$ (*via* ATR–FTIR analysis), were used to best fit the data *via* the modified Henderson–Hasselbalch equation and determine dissociation parameters (p$K_a$ and $B$) (see Table 1).

### 3.6. Molecular-level length scales

To understand the molecular picture of dissociation process in AA–PEGDA series, we used four relevant molecular-level length scales, including 1) the average distance between dissociated charged groups in a swollen polymer ($r_c$, subscript $_c$ notes charged groups), (2) the average distance between salt ions in an external solution ($r_{ion}$), the corresponding (3) Bjerrum length ($l_B$) and (4) the Debye screening length ($r_D$) in the system.

The average distance between dissociated charged groups in a swollen polymer ($r_c$) was estimated using effective ion-exchange capacity (eIEC) and equilibrium water swelling ($w_u$, $\phi_w$) by assuming the uniform volumetric distribution of charged groups in sorbed water in a swollen polymer as:[16,18,51,52]

$$r_c\,[\text{Å}] = \left(\frac{w_u \cdot 1000}{\rho_w \cdot \text{eIEC} \cdot \phi_w \cdot N_A}\right)^{\frac{1}{3}} \times 10^8 \quad (16)$$

where eIEC is the concentration of dissociated charged groups in the dry polymer (from eqn (7) and (8) in Section 3.1), $w_u$ is the water uptake of the polymer (g of sorbed water/g of a dry polymer), $\rho_w$ is the water density (1 g $cm^{-3}$), $\phi_w$ is water volume fraction ($cm^3$ of sorbed water/$cm^3$ of a swollen polymer), and $N_A$ is the Avogadro number ($6.022 \times 10^{23}$). In this simple first approximation, a charged group (in the polymer) and a salt ion (in an external solution) in a system are treated as a point charge, consistent with the theoretical[53–58] and experimental observations.[18,52,59] Note that we also calculated the average distance between dissociated charged groups ($r_{c,eff}$) in a polymer and the distance between salt ions in an external solution ($r_{ion,eff}$) assuming a spherical ion and details are discussed in Sections S3 and 4.5.

The average distance between dissociated charged groups in a dry polymer ($r_{c,dry}$) is calculated by assuming the uniform volumetric distribution of charged groups in the polymer as:

$$r_{c,dry}[\text{Å}] = \left(\frac{1000}{\rho_p \cdot \text{eIEC} \cdot N_A}\right)^{\frac{1}{3}} \times 10^8 \quad (17)$$

where $\rho_P$ is the polymer density [g $cm^{-3}$].

NaCl and NaOH are two salts used this study. NaCl concentration in an external solution ($C_{Nacl}$ [M]) varies from 0 M (DI water) to 1 M (*i.e.*, 0 M, 0.01 M, 0.1 M, and 1 M). The added amount of NaOH ($x_{NaOH}$ [mequiv. per g]) for titration varies from 0 to mIEC [mequiv. per g] of a polymer. The NaOH concentration ($C_{NaOH}$ [M]) is estimated as:

$$C_{NaOH}[\text{M}] = \frac{m_d}{x_{NaOH} \cdot 1000 \cdot V_s} \quad (18)$$

where $m_d$ is the dry mass of the polymer coupon [g] and $V_s$ is the volume of the external solution (0.1 L).

The total external salt concentration ($C_s$) is the sum of NaCl and NaOH concentrations ($C_s = C_{Nacl} + C_{NaOH}$). As all salts fully dissociate in water, ion concentration ($C_i$) can be expressed as $C_i = 2{\cdot}C_s$. Since the added NaOH amount for titration is very small (0–0.003 M) in this study, the total external salt concentration ($C_s$) is dominantly dependent on the NaCl concentration (0–1 M) in the external solutions (see Table S3–5). Thus, the average distance between salt ions in the external solution ($r_{ion}$) is calculated by assuming the uniform volumetric distribution

of salt ions in the external solution as:

$$r_{\text{ion}}\,[\text{Å}] = \left(\frac{1000}{C_s \cdot N_A}\right)^{\frac{1}{3}} \times 10^8 \tag{19}$$

Bjerrum length ($l_B$) is the separation distance at which the electrostatic interaction energy between two point charges, such as the charged group in a polymer and a nearby mobile ion in an external solution in our system, becomes equal to the natural energy scale, *i.e.*, thermal energy ($kT$).[52,54,57,59,60] If the separation distance ($r$) between the charged group in a polymer and the nearby mobile ion in an external solution is smaller than the Bjerrum length ($r < l_B$), the electrostatic interaction energy exceeds the thermal energy. Under these conditions, the charged group and ion remain strongly associated, which inhibits dissociation. If the separation distance ($r$) between the charged group and the mobile ion exceeds the Bjerrum length ($r > l_B$), the electrostatic interaction energy is lower than the thermal energy. As a result, the ion can dissociate (escape) from the charged group and move freely, behaving like a non-interacting species (promoting dissociation). Thus, the Bjerrum length ($l_B$) serves as a measure of the strength of electrostatic interaction energy between a charged group in a polymer and a surrounding ion in an external solution, and is expressed as:[18,52,54,57,59–61]

$$l_B\,[\text{Å}] = \frac{e^2}{4\pi\varepsilon_p\varepsilon_0 k_B T} \tag{20}$$

where $e$ is electrostatic charge ($1.60218 \times 10^{-19}$ C), $\varepsilon_p$ is the dielectric constant of the polymer, $\varepsilon_0$ is the vacuum permittivity ($8.8542 \times 10^{-12}$ F m$^{-1}$), $k_B$ is the Boltzmann constant ($1.38065 \times 10^{-23}$ J K$^{-1}$), and $T$ is an absolute temperature [K]. For AA–PEGDA series, $\varepsilon_p$ of a swollen polymer is calculated using the Bruggeman effective medium model[62–65] and the details will be discussed in Section 3.7.

Debye screening length ($r_D$) of a system characterizes the distance over which the electrostatic interaction energy from a charged group in a polymer is effectively reduced and attenuated by the surrounding mobile ions in an external solution.[52,53,60,61] If the separation distance ($r$) between a charged group in the polymer and the surrounding mobile ion in the external solution is smaller than the Debye screening length ($r < r_D$), the electrostatic interaction energy by the charged group exceeds the thermal energy ($kT$) and significantly affects the redistribution of nearby mobile ions. As a result, local electroneutrality is not preserved within this range. If the separation distance ($r$) between the charged group and the mobile ion exceeds the Debye screening length ($r < r_D$), the electrostatic interaction energy by the charged group is substantially reduced due to screening by the redistributed mobile ions in the solution. Thus, electroneutrality is preserved at the distance exceeding the Debye screening length ($r_D$). The Debye screening length ($r_D$) is expressed as:

$$r_D\,[\text{Å}] = \sqrt{\frac{\varepsilon_p\varepsilon_0 kT}{N_A e^2 \sum_{i=1}^{n} C_i z_i^2}} \tag{21}$$

where $\sum_{i=1}^{n} C_i z_i^2$ is determined as:

$$\sum_{i=1}^{n} C_i z_i^2 = 2 \cdot I \tag{22}$$

where $I$ is the ionic strength of the external solution as:

$$\begin{aligned} I &= \frac{1}{2}\left[C_{Na^+} \times (+1)^2 + C_{Cl^-} \times (-1)^2 + C_{OH^-} \times (-1)^2\right] \\ &= C_S \end{aligned} \tag{23}$$

### 3.7. Dielectric constant ($\varepsilon_p$) in a hydrated polymer

Dielectric constant ($\varepsilon$) of a material describes the polarizability of dipoles within the material under an electric field compared to a vacuum.[33,66] High dielectric medium like water ($\varepsilon_w \sim 78.2$) promotes salt dissociation, because water molecules can readily polarize and stabilize the electrostatic charges of the dissociated ions. Generally, as the dielectric constant of a material increases, dissociation is more pronounced, significantly influencing the electrostatic phenomena in a system. Thus, reasonable estimation of the dielectric constant ($\varepsilon_{p,\text{swollen polymer}}$) in a swollen polymer is required to understand the dissociation behavior in our AA–PEGDA polymers. For this purpose, we used the symmetric Bruggeman effective medium model which calculates dielectric constant of a heterogeneous material with a percolation threshold ($\phi_c \sim 0.3$) as:[62–65]

$$\begin{aligned} &\phi_w\left(\frac{\varepsilon_w - \varepsilon_{p,\text{swollen polymer}}}{\varepsilon_w + 2 \cdot \varepsilon_{p,\text{swollen polymer}}}\right) \\ &\quad + \phi_p\left(\frac{\varepsilon_{p,\text{dry polymer}} - \varepsilon_{p,\text{swollen polymer}}}{\varepsilon_{p,\text{dry polymer}} + 2 \cdot \varepsilon_{p,\text{swollen polymer}}}\right) \\ &\quad = 0 \end{aligned} \tag{24}$$

where $\phi_w$ is the water volume fraction of a swollen polymer, $\phi_p$ is the polymer volume fraction, and $\varepsilon_{p,\text{dry polymer}}$ is the dielectric constant of the dry polymer ($\sim$12).[18,52,67,68] We chose the Bruggeman model because our 10-2 AA–PEGDA network shows interconnected water domain in the swollen polymer, and comparable water content ($\phi_w$ = 0.30–0.54) above the percolation threshold of 0.3 described in the Bruggeman model. We used the $\varepsilon_{p,\text{dry polymer}}$ values from similar AA- and PEGDA-based polymers in the literature.[18,52,59] Also, dielectric constant of aqueous NaCl (aq) solution, $\varepsilon_w(C_s)$, is adjusted as a function of external salt concentration as:[69–73]

$$\varepsilon_w(C_s) = \varepsilon_{w,0} + \sum_{j=1}^{5} \theta_j^{EC} C_s^{j/2} \tag{25}$$

where $\varepsilon_{w,0}$ is the dielectric constant of pure water (78.2), $\theta_j^{EC}$ is

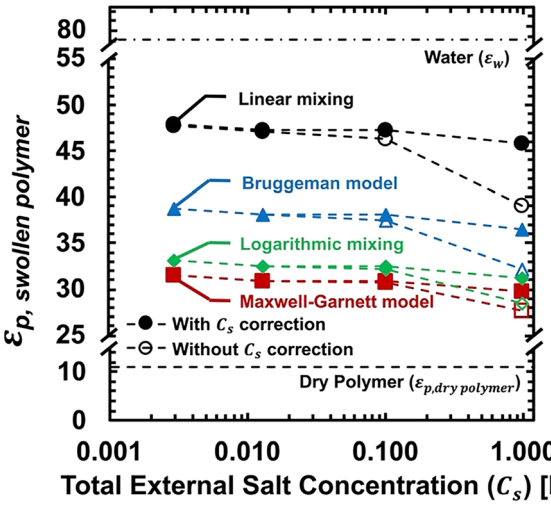


Fig. 2 Dielectric constant ($\varepsilon_{p,swollen\ polymer}$) of swollen 10-2 AA-PEGDA network *via* different estimation methods with and without adjusting the external salt concentration ($C_s$) (at the highest pH = 12). Dashed lines are used to guide the eyes.

an empirical parameter ($\theta_1^{EC} = \theta_4^{EC} = \theta_5^{EC} = 0$, $\theta_2^{EC} = -16.2$, and $\theta_3^{EC} = 3.10$), and $C_s$ is the external salt concentration [M].

For comparison, we also used other representative methods to estimate the dielectric constant of a swollen AA–PEGDA polymer (see Fig. 2 and Table S3) and recorded the influence of different dielectric constant range on our dissociation analysis (see Fig. S20). The simplest linear mixing rule assumes the volume additivity between the polymer and sorbed water in the swollen polymer as:[18,52,62,74]

$$\varepsilon_{p,swollen\ polymer} = (1 - \phi_w)\cdot\varepsilon_{p,dry\ polymer} + \phi_w\cdot\varepsilon_w \quad (26)$$

The linear mixing rule is reported to well estimate the dielectric properties of hydrated Nafion® which shows strong phase separation between the sorbed water and the polymer.[62,75] The logarithmic mixing rule also expresses the dielectric constant of a swollen polymer using $\phi_w$ and $\phi_p$ (= $1 - \phi_w$) as:[76,77]

$$\log(\varepsilon_{p,swollen\ polymer}) = (1 - \phi_w)\cdot\log(\varepsilon_{p,dry\ polymer}) + \phi_w\cdot\log(\varepsilon_w) \quad (27)$$

These two simple mixing rules are useful as a first approximation when the detailed information of polymer–water interaction is limited.

On the other hand, the Maxwell–Garnett model predicts the dielectric constant of a heterogenous material as:[62,69,78–80]

$$\frac{\varepsilon_{p,\ swollen\ polymer} - \varepsilon_{p,\ dry\ polymer}}{\varepsilon_{p,\ swollen\ polymer} + 2\cdot\varepsilon_{p,\ dry\ polymer}} = \phi_w\left(\frac{\varepsilon_w - \varepsilon_{p,\ dry\ polymer}}{\varepsilon_w + 2\cdot\varepsilon_{p,\ dry\ polymer}}\right) \quad (28)$$

This model describes the cases where water is dilute and not continuous in a system.

In Fig. 2, we showed estimated dielectric constants of swollen 10-2 AA–PEGDA network *via* four different methods with and without adjusting the external salt concentration ($C_s$) (also see Table S3). Overall, as external salt solution concentration increases, the dielectric constant of a system decreases slightly. The linear mixing rule *via* volume additivity leads to a higher dielectric constant range, since the linear mixing rule assumes the ideal mixing (of polymer and sorbed water) and does not consider geometric factors. Between 0–0.01 M NaCl (aq) concentration range, dielectric constants with and without adjusting the external salt concentration ($C_s$) are similar to each other. However, as the salt concentration increases between 0.1 M and 1 M NaCl (aq) solutions, increasing salt concentration further decreases the dielectric constants, and the difference becomes more obvious. In this study, we mainly used the dielectric constants estimated by the Bruggeman effective medium model with the external salt concentration ($C_s$) adjustment to describe the dissociation.

Using the dielectric constant ranges *via* different methods, we compared the four relevant length scales ($r_c$, $r_{ion}$, $l_B$, and $r_D$) in Fig. S20 and Tables S4 and S5. As the dielectric constants *via* different methods slightly decreases, Bjerrum length ($l_B$) slightly increases and Debye screening length ($r_D$) decreases, respectively (see eqn 20 and 21) as expected. However, regardless of the slight variations in the dielectric constants, the relative order of these length scales are consistent in our dissociation analysis, and details will be discussed in Section 4.5.

# 4. Results and discussion

## 4.1. Degree of ionization (α) before titration

To describe the complete picture of the dissociation process in AA–PEGDA series, we quantified the degree of ionization (α) in a polymer before adding a strong base (*i.e.*, NaOH in this study). Weakly acidic, carboxylic acid (COOH) groups in acrylic acid (AA) monomer slightly dissociate (ionize) in water and NaCl (aq) solution as:

$$R\text{–}COOH + H_2O \rightleftarrows R\text{–}COO^- + H_3O^+ \quad (29)$$

Consequently, carboxylate anion (R–$COO^-$) and hydronium cation ($H_3O^+$) are formed, lowering the pH of the solutions (AA monomer's p$K_a$ is 4.24–4.60 in a dilution condition[26,27,30,81,82]).

Before soaking an AA–PEGDA polymer coupon, in different external salt (NaCl) concentrated solutions of this study, *i.e.*, 0 M (DI water), 0.01 M, 0.1 M and 1 M NaCl (aq) solutions, the solution pH values were in the range of pH = 5.7–6.3 (with a variability <2–3%) regardless of the external NaCl concentrations. The solution pH values are closer but slightly lower than pH = 7 because of an equilibrium amount of dissolved carbon dioxide ($CO_2$) in water (see Section 2.4). $CO_2$ (g) from air dissolves in water to form a carbonic acid ($CO_2$ (g) + $H_2O \rightleftarrows H_2CO_3$ (aq)). The carbonic acid can partially dissociate ($H_2CO_3$ (aq) + $H_2O \rightleftarrows HCO_3^-$ + $H_3O^+$), generating a bicarbonate anion ($HCO_3^-$) and a hydronium cation ($H_3O^+$), and thus, lowering

the pH of the water. The water in equilibrium with atmospheric $CO_2$ (g) exhibits a moderately acidic pH of 5.65.[23,39,42,43] Our measured pH ranges (pH ~ 6) in the different NaCl (aq) solutions are in a similar range as those in the literature. To minimize the pH changes originating from the dissolved $CO_2$ in water during our experiments, DI water used for pH titration and salt solution preparation was equilibrated with air in ambient temperature for 24 h, and thus reached an equilibrium amount of dissolved $CO_2$ in the water, following the previously reported procedures.[74]

Note that the presence of neutral NaCl salt in water (as the different external NaCl (aq) solutions in this study) does not influence the acidity or basicity of the solution and thus does not change the solution pH. However, the added ions ($Na^+$ and $Cl^-$) dissociated from the NaCl salt increase the overall ionic strength of the external solution. External salt effects from the increased ionic strength can affect the dissociation process ($\alpha$ and $pK_a$) in weakly charged polymers, such as in AA–PEGDA series. Detailed discussion on the effects of external salt conditions on dissociation will be made in Section 4.5.

For pre-titration study, an AA–PEGDA polymer coupon was soaked in different external salt solutions of varied NaCl concentrations (0 M, 0.01 M, 0.1 M and 1 M NaCl (aq) solutions) to reach equilibrium without adding a strong base (NaOH). If a small fraction of dissociable charged (COOH) groups dissociates in weakly acidic AA–PEGDA series, the $H_3O^+$ released from the polymer lowers the pH in the external solution.[24] As the extent of dissociation to $COO^-$ groups increases, the resulting pH change in the solution becomes more pronounced. By recording the pH change in the solutions over time (see Fig. 3a), we determined pre-titration degree of ionization ($\alpha$) of the polymer using eqn (9) as shown in Fig. 3b.

Fig. 3a shows the effects of polymer composition (mIEC = 0–4 mequiv. per g, PEGDA cross-linker length, $n$ = 10 and 13) and external salt concentrations (0 M, 0.01 M, 0.1 M and 1 M NaCl (aq)) on the pre-titration pH change in the external solution after 2 days of film immersion (also see Fig. S3 and S4). For comparison, cross-linked PEGDA network films (10–0 and 13–0) without any dissociable charged (COOH) groups (*i.e.*, mIEC = 0 mequiv. per g) are shown as controls. In the absence of any dissociable charged groups in the polymers, the solution pH values contacting the PEGDA network films do not change over time and remain nearly constant (pH ~ 6) as expected. This is anticipated for non-charged PEGDA networks (thus, degree of ionization, $\alpha$ = 0).

On the other hand, in AA–PEGDA series, the extent of solution pH changes over time shows a distinct trend as a function of polymer composition (mIEC and $n$) and external salt concentrations ($C_s$). First, as mIEC increases from 0 mequiv. per g to 4 mequiv. per g (other conditions are the same in a fixed PEGDA cross-linker length, $n$ and in a fixed external NaCl concentration), the extent of pH change is greater with increasing mIEC due to the increased amount of dissociable charged (COOH) groups in the polymers. The more dissociable charged (COOH) groups in the polymers lead to the higher $H_3O^+$ concentration in the solution after partial dissociation. The higher $H_3O^+$ concentration results in a lower pH in the solution.

Secondly, as PEGDA cross-linker length ($n$) increases from $n$ = 10 to $n$ = 13 (other conditions are identical in a fixed mIEC and a fixed external NaCl concentration), the extent of the pH changes is slightly larger within the uncertainty of a measurement, because of higher water swelling in a looser network in 0.01 M to 1.0 M NaCl (aq) solutions. In DI water (0 M NaCl (aq) solution), the difference (of the solution pH changes) is almost negligible due to suppressed dissociation, but in 0.01 M to 1 M NaCl (aq) solutions, the difference between $n$ = 10 and $n$ = 13 is more obvious although the data remain within the uncertainty of a measurement. In general, a looser network with a longer cross-linker exhibits a higher water swelling with a lower cross-linking density. A water-rich, high dielectric environment in the looser network favors more dissociation. High water swelling also reduces the electrostatic repulsion between dissociated charged groups by increasing the distance between the charged groups, and thus, promotes more dissociation. Both effects (in the looser network) lead to the increased amount of dissociated $COO^-$ groups, lowering the pH in the external solution. This trend is likely to be similar, but the difference between $n$ = 10

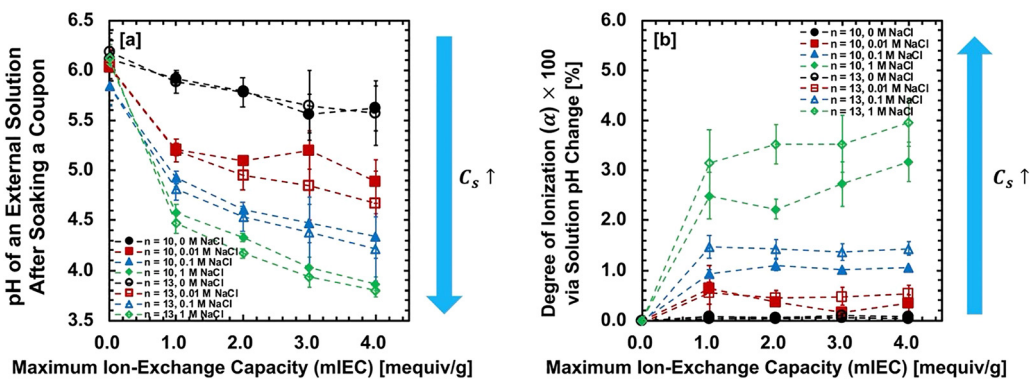


Fig. 3 [a] pH of an external solution after soaking AA–PEGDA coupon in different NaCl (sq) solutions (0–1 M NaCl (aq)) for 2 days before titration. No strong base (NaOH) was added. [b] Pre-titration degree of ionization ($\alpha$) × 100 [%] *via* solution pH change. Arrows show total external salt concentration ($C_s$). Dashed lines are used to guide the eyes. Error bars are included.

and $n$ = 13 series in the DI water is almost negligible. This is due to the suppressed dissociation *via* the enhanced electrostatic repulsion between charged groups in dilute conditions, because the electrostatic screening effects by the added external salt (NaCl) are ruled out. Detailed discussion will be made in Section 4.5.

Thirdly, in a fixed polymer composition (mIEC and $n$ are fixed), as the external NaCl concentration increases between 0 M and 1 M NaCl (aq) solutions, the extent of the solution pH changes is greater due to the increased electrostatic screening effects by the added external salts. Increased amounts of the external salts screen and modulate the electrostatic repulsion between dissociated charged groups, leading to more dissociation. More dissociation in the higher salt concentrated solutions results in a larger pH decrease (Detailed discussion in Section 4.5).

Fig. 3b summarizes the pre-titration degree of ionization ($\alpha$) determined by the solution pH changes in Fig. 3a (also see Fig. S5). The extent of dissociation degree ($\alpha$) before adding a strong base (NaOH) is very small (0–4%) in the different NaCl (aq) solutions. Although the extent of dissociation degree ($\alpha$) is very small, the dissociation behavior shows consistent trends as a function of polymer composition (mIEC and $n$) and external salt concentrations ($C_s$). In general, as mIEC increases, PEGDA cross-linker length ($n$) increases, and external salt concentration ($C_s$) increases (see Fig. 4), the degree of ionization ($\alpha$) slightly increases as expected. In the 0 M NaCl (aq) solutions, the pre-titration dissociation degree is negligible ($\alpha$ = 0.05% ± 0.02%) regardless of polymer composition.[22,23,39] As the external NaCl concentration increases, the degree of ionization ($\alpha$) slightly increases up to $\alpha$ = 4% because of the enhanced electrostatic screening effects by the added external salts as shown in Fig. 4 (also see Fig. S6). Overall, our pre-titration dissociation analysis supports the assumption that the major dissociation in AA–PEGDA series arises as a strong base (NaOH) is added for titration.[24–28] The pre-titration results also provide a reference point for our subsequent analysis.

### 4.2. pH titration curve

In this study, we mainly focused on the representative chemical structure of AA–PEGDA series, *i.e.*, 10-2 AA–PEGDA network (mIEC = 2 mequiv. per g and PEGDA cross-linker length $n$ = 10) to investigate the effect of external salt concentrations on the dissociation behavior ($\alpha$ and p$K_a$) during titration. The 10-2 network was selected because its IEC (eIEC = 0–2 mequiv. per g) and water swelling ($\phi_w$ = 0.30–0.54) ranges are most relevant to other commercially available and/or widely studied polyelectrolyte membranes.[33–38] Using the fixed 10-2 network film, we recorded the pH *vs.* the added amount of a strong base (NaOH) in the different NaCl (aq) solutions (0–1 M) as shown in Fig. 5.

In a strongly acidic polymer, all strong acid groups dissociate in water and NaCl (aq) solution ($HA + H_2O \rightleftharpoons H_3O^+ + A^-$).[24] During titration with a strong base (*e.g.*, NaOH), the pH in the solution exhibits a plateau and remains relatively constant until an equivalence point is reached. An equivalence point represents the stoichiometric balance where the amount of added $OH^-$ equals the amount of $H_3O^+$ released from the polymer ($[OH^-] = [H_3O^+]$). Beyond the equivalence point, the excess amount of $OH^-$ ($[OH^-]$) causes a steep increase in the solution pH, as the titration reaches its completion point.

In contrast, weakly acidic polymers, such as AA–PEGDA series in this study, exhibits different behavior in pH titration because their acidic groups dissociate partially ($HCOOH + H_2O \rightleftarrows HCOO^- + H_3O^+$). The acid dissociation constant ($K_a$) is defined as:[24]

$$K_a = \frac{[H_3O^+] \cdot [A^-]}{[HA]} \quad (30)$$

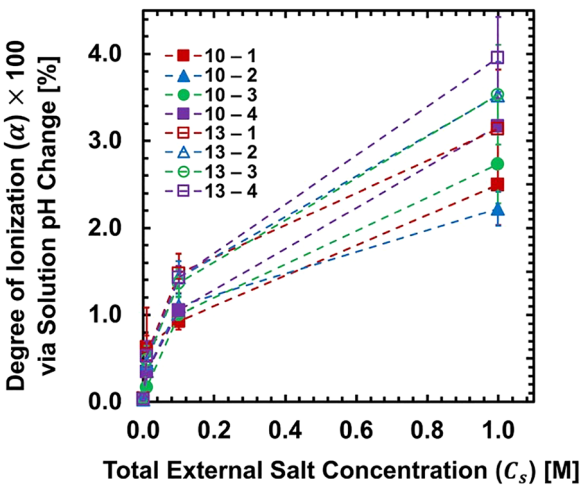


Fig. 4 Pre-titration degree of ionization ($\alpha$) × 100 [%] of AA–PEGDA series *vs.* total external salt concentration ($C_s$). Dashed lines are used to guide the eyes. Error bars are included.

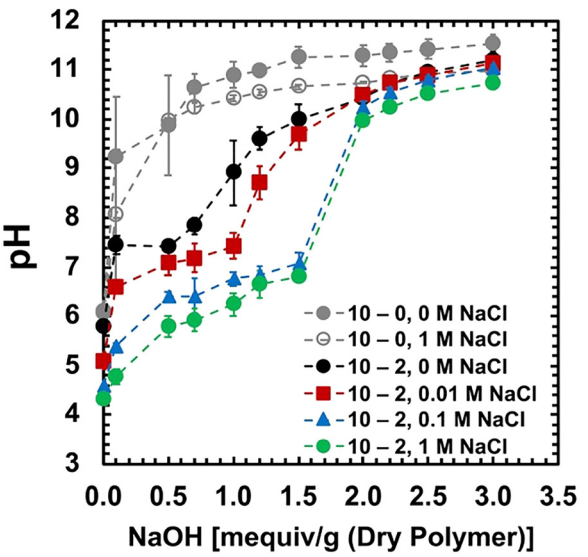


Fig. 5 pH *vs.* added NaOH amount [mequiv. per g] in PEGDA (10–0, mIEC = 0 mequiv. per g) and 10-2 AA–PEGDA networks in different NaCl (aq) solutions (0–1 M NaCl (aq)). Dashed lines are used to guide the eyes. Error bars are included.

and can be related to pH (= $-\log[H_3O^+]$) as:

$$[H_3O^+] = \frac{K_a \cdot [HA]}{[A^-]} \quad (31)$$

As a strong base (NaOH) is added, it reacts with the weak acid to form its conjugate salt (NaA) (HA + NaOH $\rightleftharpoons$ NaA + $H_2O$). This reaction initially reduces the amount of dissociated $A^-$ ($[A^-]$). To preserve equilibrium stoichiometry, additional HA dissociates into $A^-$, leading to a decrease in [HA] and an increase in $[A^-]$. Consequently, the pH increases as $[H_3O^+]$ decreases. At the halfway point of the titration, one half of the original HA has dissociated, so the concentrations of HA and $A^-$ are equal ($[HA]_{1/2} = [A^-]_{1/2}$). This corresponds to a degree of ionization ($\alpha$) of 0.5. The negative logarithm of apparent acid dissociation constant in a polymer, p$K_a$ is determined as the negative logarithm of the hydronium concentration ($[H_3O^+]$) at the halfway point ($PH_{1/2}$) as:

$$pK_a = pH_{1/2} \quad (32)$$

Prior to the titration (before adding the strong base (NaOH)), the fraction of dissociated $A^-$ in the polymer is assumed to be very small. This is the case with the 10-2 AA–PEGDA network as discussed in Section 4.1. The pre-titration dissociation degree ($\alpha$) is very small ($\alpha$ = 0–4%) for AA-PEGDA series in the different NaCl (aq) solutions. Beyond the halfway point, continued addition of the strong base drives further dissociation of the remaining HA until its neutralization is complete ($\alpha$ = 1), resulting in an increase in the solution pH. As the titration is completed, the excess amount of $OH^-$ ($[OH^-]$) governs the solution pH.

Our weakly acidic 10-2 AA–PEGDA network shows similar pH titration behavior as shown in Fig. 5. As a reference, pH titration curves of cross-linked PEGDA network (10–0) without any dissociable charged groups (mIEC = 0 mequiv. per g) in different NaCl (aq) solutions are shown. Without any dissociable COOH groups, PEGDA network shows steeper pH increase in the solution in an early stage in 0 M and 1 M NaCl (aq) solutions (other NaCl (aq) solutions also yield similar pH titration curves but are not shown for brevity). This is expected because the added NaOH does not need to neutralize the uncharged PEGDA network and thus directly contributes to increasing the solution pH.

On the other hand, in the 10-2 AA–PEGDA network with dissociable COOH groups (mIEC = 2 mequiv. per g), as the strong base (NaOH) is added, the amount of dissociated $COO^-$ groups in the polymer increases gradually. The added NaOH titrates (neutralizes) the polymer and thus the solution pH increases correspondingly. As the external NaCl concentration increases from 0 M to 1 M, the pH titration curves shift to lower pH ranges because of the enhanced electrostatic screening effects by the added external salts.[53,61,81,83,84] Increasing amount of the external salts modulates and reduces the electrostatic repulsion between charged groups in the polymer, promoting dissociation and thus decreasing p$K_a$. The downshifting trend with the increasing external salt concentration represents the promoted dissociation (thus, decreased p$K_a$) by the added external salts. While the downshifting trend is more obvious between 0–0.1 M NaCl (aq) solutions, the shifting trend after 0.1 M NaCl (aq) becomes much smaller between 0.1–1.0 M NaCl (aq) solutions. This is because the electrostatic repulsion between charged groups is effectively screened in and after adding 0.1 M NaCl (aq) solution. Details will be discussed with respect to relevant, molecular-level length scales in Section 4.5. When the added amount of NaOH equals the total amount of dissociable charged groups (mIEC = 2 mequiv. per g) in the 10-2 network, titration approaches its completion point (the degree of ionization, $\alpha$ = 1).

In addition, during the titration, we performed ATR–FTIR analysis to measure the concentrations of dissociable COOH and dissociated $COO^-$ groups in the polymer phase (see Section S2 and Fig. S11). Fig. S12 and S13 show the concentrations of dissociable COOH (at 1700 $cm^{-1}$) and dissociated $COO^-$ groups (at 1575 $cm^{-1}$ and 1400 $cm^{-1}$) in the polymer *vs.* added NaOH amount, following the methods reported previously.[23,26,39,50] As the pH increases (with the increasing NaOH amount), the absorbance intensities (and the areas under the curves) of the dissociated $COO^-$ groups (at 1575 $cm^{-1}$ and 1400 $cm^{-1}$) also increase (see Fig. S12a–d and S13a and b), while the areas under the curves of the dissociable COOH groups (at 1700 $cm^{-1}$) decrease (see Fig. S13c and d). Note that the absorbance intensities at 1100 $cm^{-1}$ (ether C–O–C stretching from ethylene oxide (EO) groups in PEGDA cross-linker) remain almost constant as expected (see Fig. S12e and f). This confirms that no chemical degradation occurs during the titration.

### 4.3. Degree of ionization ($\alpha$) and p$K_a$ *via* the modified Henderson–Hasselbalch equation

We reported the degree of ionization ($\alpha$) and p$K_a$ values of 10-2 AA–PEGDA network in different NaCl (aq) solutions (0–1 M) *via* (1) potentiometric (POT) titration of the network film with the strong base (NaOH) and (2) subsequent ATR–FTIR analysis. Through integrating the dissociation data in both solution phase (*via* POT titration) and polymer phase (*via* ATR–FTIR analysis) together, we can rigorously probe the dissociation process and quantify the dissociation parameters ($\alpha$ and p$K_a$) of the polymers. We used the modified Henderson–Hasselbalch equation to fit the data and describe the physical picture of the dissociation in the polymers.

Fig. 6a shows the degree of ionization ($\alpha_{pH}$) *vs.* pH data of 10-2 network in different NaCl (aq) solutions *via* POT titration whereas Fig. 6b exhibits the $\alpha_{IR}$ *vs.* pH results *via* ATR–FTIR analysis. In both figures, symbols are experimental data while solid lines are the best fit through the data using the modified Henderson–Hasselbalch equation. As the external pH increases between 3–12, the degree of ionization ($\alpha$) increases between 0–1, following the modified Henderson–Hasselbalch equation. At pH > 10–11, the 10-2 network is fully dissociated ($\alpha$ = 1). Overall, both methods (POT titration and ATR–FTIR analysis) show similar $\alpha$ *vs.* pH trends. This confirms that both methods faithfully reflect the dissociation process in both solution and polymer phases (also see Fig. S14). Also, our $\alpha$ *vs.* pH data are

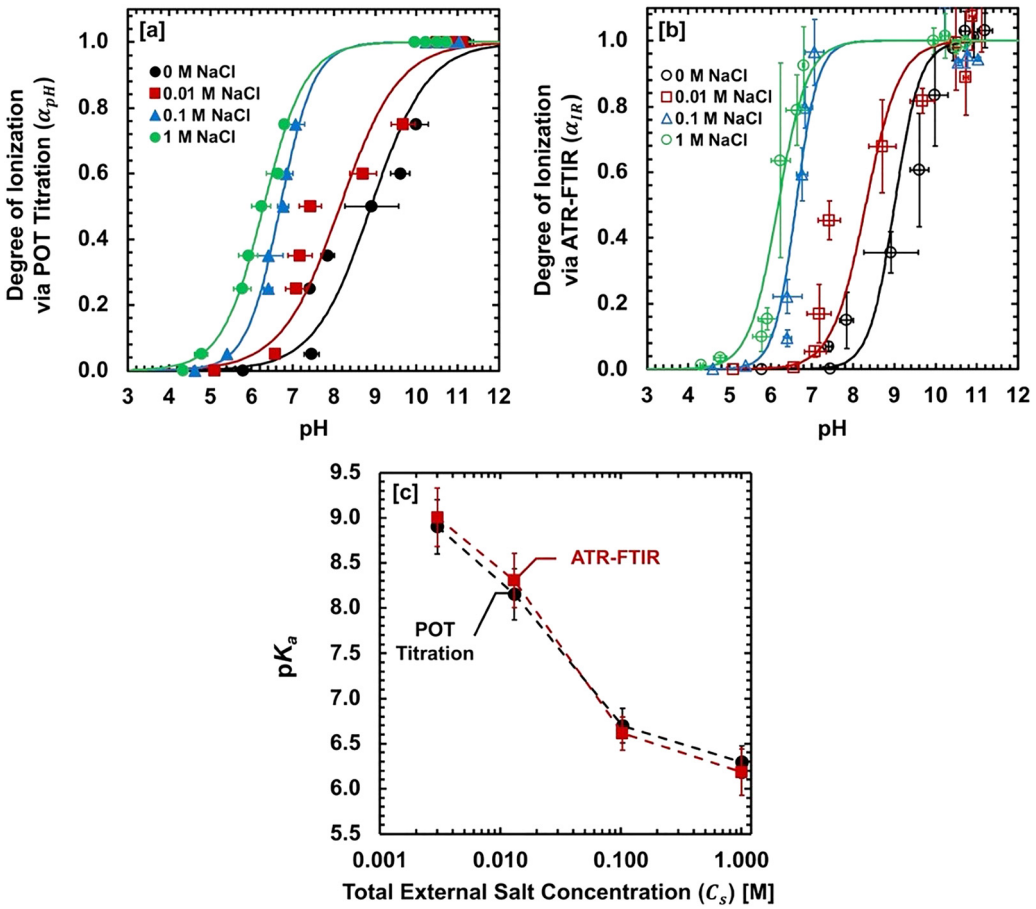


Fig. 6 [a] Degree of ionization ($\alpha_{pH}$) *vs.* pH of 10-2 AA–PEGDA network in different NaCl (aq) solutions (0 M to 1 M NaCl (aq)) *via* POT titration. Symbols are experimental data. Solid lines are the best fit using the modified Henderson–Hasselbalch equation. [b] Degree of ionization ($\alpha_{IR}$) *vs.* pH *via* ATR–FTIR analysis. [c] p$K_a$ *vs.* total external salt concentration ($C_s$). Dashed lines are used to guide the eyes. Error bars are included.

Table 1 p$K_a$ and $B$ values of 10-2 AA–PEGDA network in different NaCl (aq) solutions (0 M to 1 M NaCl (aq)) determined using the modified Henderson–Hasselbalch equation *via* POT titration and ATR–FTIR analysis[a]

| | NaCl Concentration in an external solution ($C_{Nacl}$) [M] | | | | | | | |
|---|---|---|---|---|---|---|---|---|
| | 0 M (DI water) | | 0.01 M | | 0.1 M | | 1 M | |
| Method | p$K_a$ | $B$ | p$K_a$ | $B$ | p$K_a$ | $B$ | p$K_a$ | $B$ |
| POT titration | 8.90 ± 0.30 | 1.59 ± 0.13 | 8.15 ± 0.28 | 1.65 ± 0.13 | 6.70 ± 0.19 | 0.95 ± 0.09 | 6.30 ± 0.18 | 1.18 ± 0.03 |
| ATR–FTIR analysis | 9.00 ± 0.33 | 0.71 ± 0.07 | 8.30 ± 0.30 | 0.94 ± 0.07 | 6.61 ± 0.18 | 0.61 ± 0.05 | 6.18 ± 0.26 | 0.82 ± 0.09 |

[a] For each measurement, an average value with a standard deviation is reported with at least three samples.

aligned well with the modified Henderson–Hasselbalch equation. This indicates that our system can be reasonably analyzed within the framework of the modified Henderson–Hasselbalch equation (eqn (15)). pH *vs.* log($\alpha$/(1 − $\alpha$)) was plotted and straight lines were found in all data sets as shown in Fig. S15. At the halfway point ($\alpha$ = 0.5), p$K_a$ value was determined using eqn (32) (see Fig. 6c). The slope of pH *vs.* log($\alpha$/(1 − $\alpha$)) plot was the fitting parameter ($B$) (see Fig. S16). The degree of ionization ($\alpha$), p$K_a$ and fitting parameter ($B$) values are summarized in Table 1.

Note that, in Fig. 6c, we used the maximum amount of added NaOH (*i.e.*, 3 mequiv. per g in this study) for the complete titration of the 10-2 network to calculate the total external salt concentrations ($C_s$) (see Section 3.6). p$K_a$ *vs.* total external salt concentration ($C_s$) plots using the different amount of added NaOH (for titration) can be found in Fig. S17.

As the external NaCl concentration increases (0–1 M), the $\alpha$ *vs.* pH curves shift to the left (see Fig. 6a and b), indicating the decreased p$K_a$ from p$K_a$ = 9 to p$K_a$ = 6 *via* both methods (see Fig. 6c). As the external NaCl concentration increases, the increased external salts modulate and screen the electrostatic repulsion between the charged groups and thus promote the dissociation. The increased electrostatic screening effects result in lowered p$K_a$ values.[81]

 

On the other hand, as the external NaCl concentration increases (0–1 M), water swelling ($\phi_w$) decreases in the polymer because of an osmotic deswelling effect. A water–reduced environment provides a lower dielectric medium, hindering dissociation and thus increasing p$K_a$.[85] Detailed discussion on the competing effects of the added external salts on the dissociation will be made in the following section (see Section 4.4).

Fig. S16 shows the fitting parameter ($B$) *vs.* external salt concentrations *via* both methods (see also Fig. S18). Fitting parameter ($B$) is the slope of dissociation curve (pH *vs.* $\log(\alpha/(1-\alpha))$). $B$ value does not have a physical origin but describes the degree of deviation from the ideal Henderson–Hasselbalch equation.[25] If $B$ = 1, dissociation curve follows the ideal Henderson–Hasselbalch equation. If B deviates from 1, some researchers relate the deviation degree with polymer composition and/or morphological features in ion-exchange resins and polyelectrolyte polymers.[44,86,87] Some reports used $B$ values as a non-ideality factor to correlate a system with respect to its ideal solution analog.[25,86] Although the physical interpretation of $B$ value in polyelectrolyte polymers remains uncertain and somewhat speculative, it is still useful to report the general trend of $B$ values observed in our 10-2 network. First, our $B$ values ($B$ = 0.6–1.7) are in a similar range of other acrylic acid (AA)-based polymers ($B$ = 1.0–2.7) in the literature.[25,27,28,44,86,87] Second, $B$ values *via* POT titration are slightly higher than those *via* ATR–FTIR analysis, reflecting differences in measurement methods as reported previously.[23,39] Thirdly, varying NaCl (aq) concentrations does not have a significant effect on $B$ values. Both methods exhibit a similar nonmonotonic dependence on external salt concentration. Similar challenges in relating $B$ values to polymer parameters and experimental conditions have also been reported in the literature.[25,27,28,44,86,87]

### 4.4. Effects of charged group content ($C_c^m$), water swelling ($\phi_w$) and external salt concentration ($C_s$) on dissociation (p$K_a$)

To understand the governing molecular variables on dissociation behavior by changing external salt concentrations in the fixed 10-2 AA-PEGDA network, we reported the effects of charged group concentration ($C_c^m$), equilibrium water swelling ($\phi_w$) and external salt concentration ($C_s$) on the dissociation parameter (p$K_a$) as shown in Fig. 7. We plot the charged group concentration ($C_c^m$) and water swelling ($\phi_w$) as a function of external salt concentration ($C_s$) because changes in the external salt concentrations ($C_s$) alter the polymer's water swelling ($\phi_w$) through osmotic deswelling effect induced by the added salts. Variations in water swelling ($\phi_w$) in turn modify the charged group concentration ($C_c^m$) in the swollen polymer. Consequently, these molecular variables ($C_c^m$, $\phi_w$, and $C_s$) are interdependent and must be considered cooperatively in the 10-2 network. (Note that, since the added NaOH amount is very

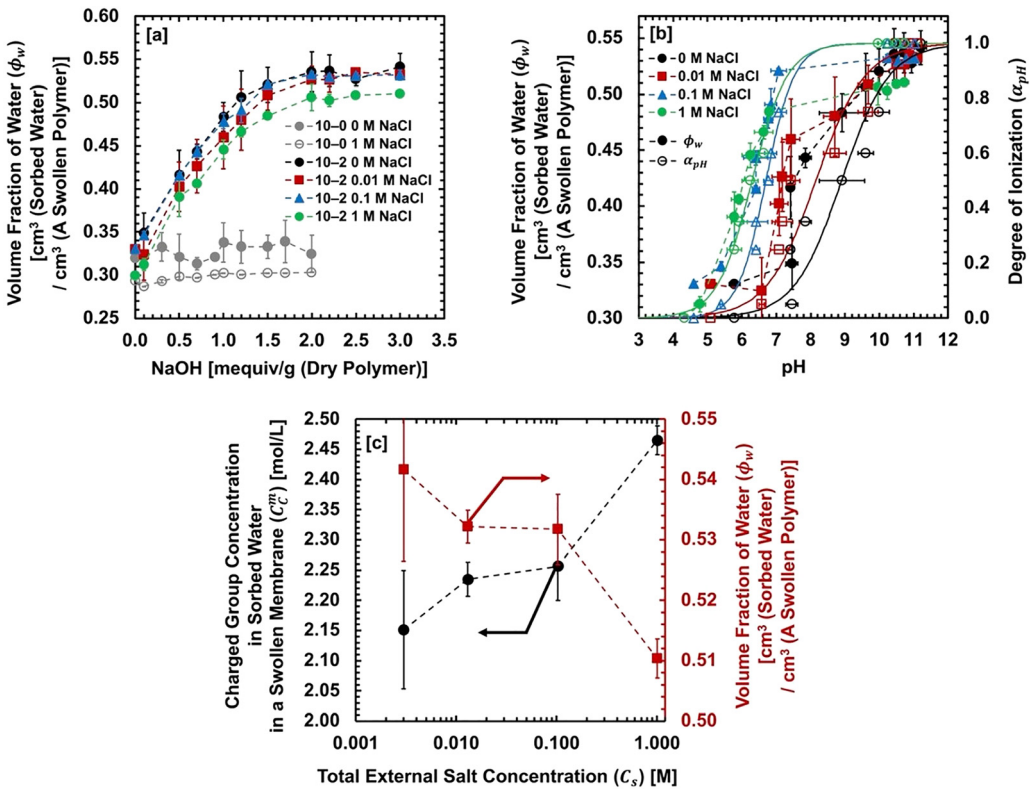


Fig. 7 [a] Water volume fraction ($\phi_w$) *vs.* added NaOH amount in different NaCl (aq) solutions (0–1 M NaCl (aq)). [b] Water volume fraction ($\phi_w$) (filled symbols) and degree of ionization ($\alpha_{pH}$) (unfilled symbols) *vs.* pH. [c] Charged group concentration in a swollen polymer ($C_c^m$) and water volume fraction ($\phi_w$) *vs.* total external salt concentration ($C_s$). Dashed lines are used to guide the eyes. Error bars are included.

small (0–0.003 M) in this study, the total external salt concentration ($C_s$) is dominantly dependent on the NaCl concentration (0–1 M) in the external solutions.)

In AA–PEGDA series, these linked molecular variables ($C_c^m$, $\phi_w$, and $C_s$) exert competing influences on the dissociation behavior ($\alpha$ and p$K_a$) in the polymers.[23] In general, (1) first, higher charged group concentration ($C_c^m$) in a polymer leads to increased water swelling ($\phi_w$). Dissociated charged groups in a polymer like to be surrounded by water to lower the free energy of a system *via* hydration, while the elastic force exerted by the polymer matrix resists the increased water sorption. As the osmotic pressure of the sorbed water reaches equilibrium with the elastic force exerted by the polymer matrix, an equilibrium water swelling is established.[88] The more dissociated charged groups are in a polymer, the higher the water swelling ($\phi_w$) is in the AA-PEGDA network. Enhanced water swelling ($\phi_w$) in a polymer network creates a water-rich, high dielectric environment that promotes dissociation. Additionally, greater water swelling increases the separation distance between the charged groups, reducing the electrostatic repulsion among the dissociated charged groups.[89] Together, both effects (*via* high water swelling) favor increased dissociation and thus a lower p$K_a$.[24] (2) Secondly, as the external salt concentration ($C_s$) increases, the increased external salts screen the electrostatic repulsion between the dissociated charged groups, thereby promoting dissociation and lowering p$K_a$.

(3) On the other hand, as the external salt concentration ($C_s$) increases, water swelling ($\phi_w$) in the polymer decreases due to an osmotic deswelling effect. An increase in external salt concentration decreases the external water concentration, leading to a lower osmotic pressure of sorbed water into the polymer. Reduced osmotic pressure difference between the external solution and the polymer results in decreased water swelling ($\phi_w$). Subsequently, a water–reduced environment offers a lower dielectric medium, hindering dissociation and thus increasing p$K_a$.[85]

Fig. 7a shows the equilibrium water swelling ($\phi_w$) of 10-2 network *vs.* added NaOH amount in different NaCl (aq) solutions. As a reference, water swelling ($\phi_w$) trends of cross-linked PEGDA network (10–0) without any dissociable charged (COOH) groups (mIEC = 0 mequiv. per g) are shown in 0 M and 1 M NaCl (aq) solutions ($\phi_w$ values in other different NaCl (aq) solutions are in between these ranges but are not shown for brevity and clarity). Without any dissociable charged groups, 10–0 network shows almost constant water swelling ($\phi_w \sim 0.29$–$0.33$) *vs.* the added NaOH amount (thus, the external pH) as expected. The 10–0 network also shows slightly decreased water swelling ($\phi_w$) with increasing external salt concentration ($C_s$) due to the osmotic deswelling.

In contrast, in the 10-2 network with dissociable charged groups (mIEC = 2 mequiv. per g), water swelling ($\phi_w$) increases *vs.* the added NaOH amount, as consistent with the pH titration curve (see Fig. 5). The water swelling ($\phi_w$) trend strongly correlates with the degree of ionization ($\alpha$) as shown in Fig. 7b as expected. As the external pH increases between pH = 4 and pH = 12, the amount of dissociated $COO^-$ groups increases (thus, $\alpha$ increases between 0–1) and water swelling ($\phi_w$) correspondingly increases ($\phi_w$ = 0.30–0.54), following the $\alpha$ *vs.* pH trend. The more dissociated charged groups are in a polymer, the higher the water swelling ($\phi_w$) is in the 10-2 network.

In the fixed 10-2 network, as the external NaCl concentration increases (0–1 M), water swelling ($\phi_w$) decreases by 6–9% because of the osmotic deswelling effect by the added external salts.[16,18,19,85] Simultaneously charged group concentration ($C_c^m$) increases by 15% (see the magnified view in Fig. 7c). (Note that we used $\phi_w$ values at the highest pH (pH = 11 $\sim$ 12) to show the extent of $\phi_w$ and $C_c^m$ changes *vs.* increased $C_s$.) This indicates that the varied external NaCl concentration (0–1 M) range in this study only slightly changes the water swelling ($\phi_w$) and charged group concentration ($C_c^m$) in the polymer. For comparison, the 10–0 network without any dissociable charged groups also shows similar slightly decreased water swelling ($\phi_w$) by 6–8% with the increased external salt concentration ($C_s$) due to the osmotic deswelling (see Fig. 7a).

These two nearly constant parameters ($\phi_w$, $C_c^m$) *vs.* the varied external salt concentration ($C_s$) indicate that these two parameters ($\phi_w$, $C_c^m$) are not the major factors for dictating the dissociation and lowered p$K_a$ in this case. Therefore, in our 10-2 network, as the external salt concentration ($C_s$) increases, the reduced electrostatic repulsion between the dissociated charged groups *via* the added external salts governs the dissociation. Thus, p$K_a$ is lowered, although higher external salt concentrations ($C_s$) slightly reduce water swelling ($\phi_w$) in the polymer (suppressing dissociation and increasing p$K_a$).

### 4.5. Molecular picture of dissociation *via* relevant length scales

To describe the molecular picture of dissociation behavior in the fixed 10-2 AA–PEGDA network in different external salt concentrations (0 M to 1.0 M NaCl (aq)), we compared four relevant molecular-level length scales in our system. Our p$K_a$ values (*via* POT titration) are plotted with respect to (1) the average distance between dissociated charged groups in a swollen polymer ($r_c$) at the highest pH = 11–12, (2) the average distance between salt ions in an external solution ($r_{ion}$), the respective (3) Bjerrum length ($l_B$) and (4) Debye screening length ($r_D$) in a system as shown in Fig. 8 and Table S5. The motivation for plotting p$K_a$ *vs.* these four length scales ($r_c$, $r_{ion}$, $l_B$, and $r_D$) comes from the fact that the electrostatic interaction originating from polymer composition ($C_c^m$, $\phi_w$) and different external salt concentration ($C_s$) governs the dissociation process. To determine the governing molecular factors on the electrostatic interaction (thus, dissociation) in our system, our system is first expressed using two representative length scales, *i.e.*, (1) the average distance between charged groups in a polymer ($r_c$) and (2) the average distance between salt ions in an external solution ($r_{ion}$). Relative standing between these two length scales with respect to each other generally determines both the strength and nature of electrostatic interaction in the system.

 

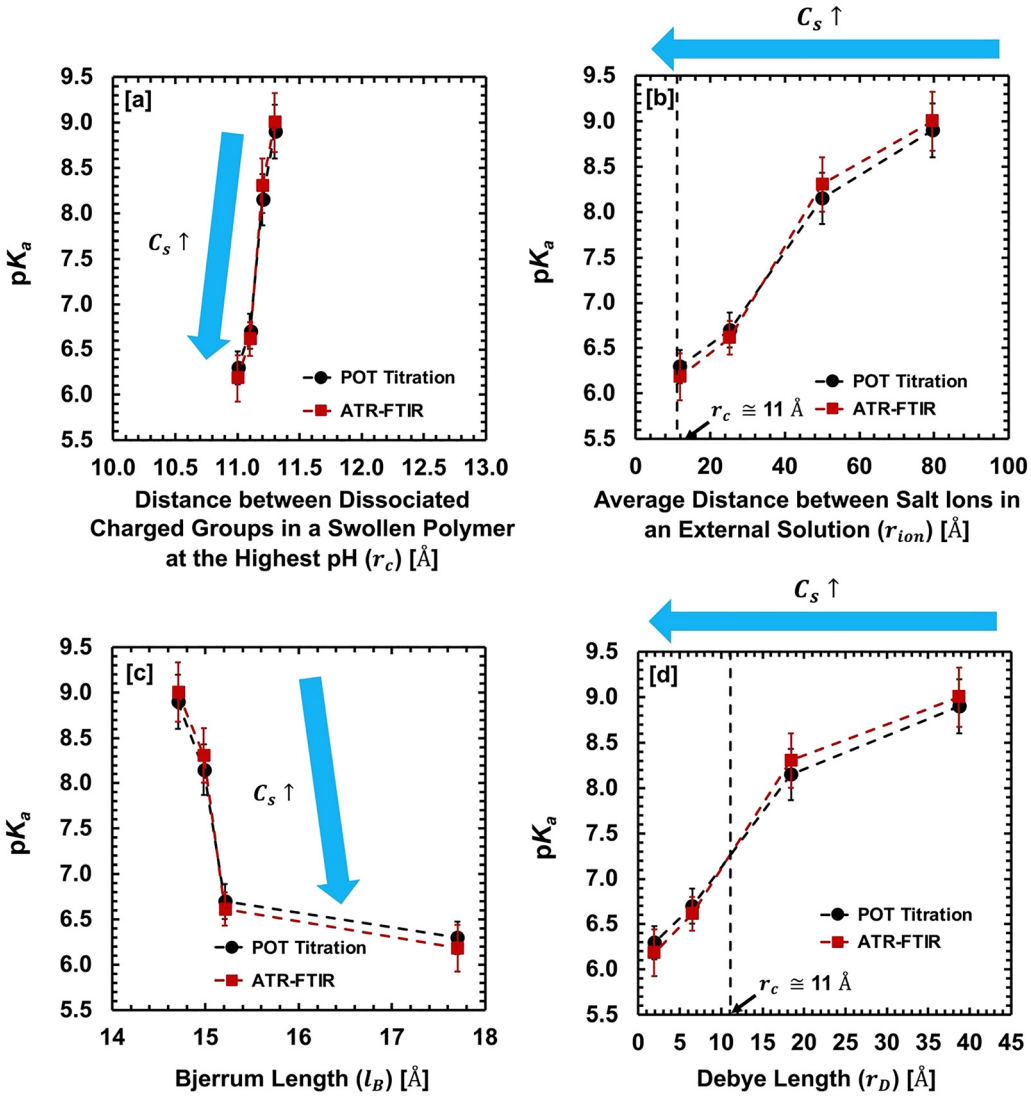


Fig. 8 p$K_a$ (*via* POT titration) *vs.* [a] the average distance between dissociated charged groups in a swollen polymer ($r_c$) at the highest pH (pH = 11–12), [b] the distance between salt ions in an external solution ($r_{ion}$), [c] Bjerrum length ($l_B$) and [d] Debye screening length ($r_D$) in 10-2 AA–PEGDA network in different NaCl (aq) solutions (0–1 M NaCl). Dashed lines are used to guide the eyes. Error bars are included.

Also, the respective (3) Bjerrum length ($l_B$) and (3) Debye screening length ($r_D$) are used to understand the electrostatic phenomena. In this system, Bjerrum length ($l_B$) is used to measure the strength of electrostatic interaction between charged groups in a polymer and surrounding mobile ions in an external solution. Debye screening length ($r_D$) indicates the distance where the electrostatic interaction exerted by the polymer's charged group is effectively screened by the external solution's mobile ions. For a comprehensive understanding, these four length scales ($r_c$, $r_{ion}$, $l_B$, and $r_D$) need to be discussed together.

First, in the lower NaCl concentration range of external salt solutions (0 M $\leq C_{Nacl} \leq$ 0.01 M), as the external NaCl concentration increases, the charged group distance in a polymer ($r_c$) at the highest pH (pH = 11–12) is in a similar range of $r_c \cong 11$ Å ($r_c$ slightly decreases from $r_c$ = 11.3 Å to $r_c$ = 11.2 Å with increasing NaCl concentration because of osmotic deswelling) (see Fig. 8a) and its corresponding Bjerrum length ($l_B$) is also in a similar range of 15 Å ($l_B$ slightly increases from $l_B$ = 14.7 Å to $l_B$ = 15.0 Å with increasing NaCl concentration) (see Fig. 8c). The charged group distance ($r_c \cong 11$ Å) is slightly shorter than the Bjerrum length ($l_B \cong 15$ Å). If the distance is shorter than the Bjerrum length ($r_c < l_B$), the electrostatic interaction energy exceeds the thermal energy ($kT$). Thus, the charged group and ion remain strongly associated, which inhibits dissociation. Both length scales ($r_c$, $l_B$) of the polymer indicate the p$K_a$ value to be in a higher range.

In the lower NaCl concentration solutions, as the external NaCl concentration increases, the average distance between salt ions in an external solution ($r_{ion}$) decreases from $r_{ion}$ = 79.6 Å to $r_{ion}$ = 50.0 Å (see Fig. 8b). The charged group distance in the polymer ($r_c \cong 11$ Å) is substantially shorter than the distance between the salt ions ($r_{ion} \cong$ 80–50 Å) in the solutions. This suggests that the concentration of external salt ions is too

low to effectively regulate the electrostatic repulsion between the polymer's charged groups. Consistently, the corresponding Debye screening length ($r_D$) range of 39–18 Å (see Fig. 8d) is longer than the charged group distance ($r_c \cong 11$ Å) but shorter than the spacing between salt ions ($r_{ion} \cong$ 80–50 Å). At a distance shorter than the Debye screening length ($r < r_D$), the electrostatic interaction energy by the polymer's charged groups exceeds the thermal energy. Thus, the electrostatic interaction energy overcomes the random thermal motion of surrounding mobile ions, influencing the rearrangement of the mobile ions. Overall, the relative order of these four length scales ($r_c < l_B \ll r_D < r_{ion}$) represents that the enhanced electrostatic interaction in dilute solutions is the dominant factor to suppress the dissociation and thus increase p$K_a$.

Note that the average distance between external salt ions ($r_{ion}$) was estimated by assuming the uniform distribution of salt ions in an external salt solution (see eqn (19)) to broadly compare salt ion distances over different salt solution concentration ranges. While the assumption of uniform salt ion distribution is more valid in higher salt concentration ranges, at lower salt concentration ranges, external salt ions can be heterogeneously distributed in a system, further increasing the average distance between external salt ions.

Secondly, in the higher NaCl concentration range of external salt solutions (0.1 M $\leq C_{Nacl} \leq$ 1.0 M), as the external NaCl concentration increases, the average charged group distance in a polymer ($r_c$) is in a similar range of 11 Å ($r_c$ slightly decreases from $r_c$ = 11.1 Å to $r_c$ = 11.0 Å with increasing NaCl concentration due to osmotic deswelling) (see Fig. 8a) and its corresponding Bjerrum length ($l_B$) is also in the range of 15–18 Å ($l_B$ slightly increases from $l_B$ = 15.2 Å to $l_B$ = 17.7 Å with increasing NaCl concentration) (see Fig. 8c). The charged group distance ($r_c \cong 11$ Å) is slightly shorter than the Bjerrum length ($l_B \cong$ 15–18 Å).

In higher NaCl concentration solutions, as the external NaCl concentration increases, the average distance between salt ions in an external solution ($r_{ion}$) decreases from $r_{ion}$ = 25.2 Å to $r_{ion}$ = 11.8 Å (see Fig. 8b). The spacing between salt ions ($r_{ion} \cong$ 25–12 Å) becomes comparable to the charged group distance ($r_c \cong 11$ Å) in the polymer. This indicates that sufficient salt ions are present to screen and modulate the electrostatic repulsion between the charged groups in the polymer. This is consistent since the Debye screening length ($r_D$) is in the range of 7–2 Å (see Fig. 8d), which is shorter than the charged group distance ($r_c \cong 11$ Å) in the polymer as well as the spacing between salt ions ($r_{ion} \cong 25 \sim 12$ Å) in the solutions ($r_D < r_c \lesssim r_{ion}$). At a distance exceeding the Debye screening length ($r > r_D$), the electrostatic interaction energy by the charged group is substantially reduced due to screening by the redistributed mobile ions in the solution. Consequently, the screened electrostatic interaction energy no longer significantly suppresses the dissociation and moves p$K_a$ to a lower value.

Overall, in the higher NaCl concentration solutions (0.1 M $\leq C_{Nacl} \leq$ 1.0 M), the relative standing of these four length scales ($r_D \ll r_c \lesssim l_B \lesssim r_{ion}$) indicates that the screened electrostatic

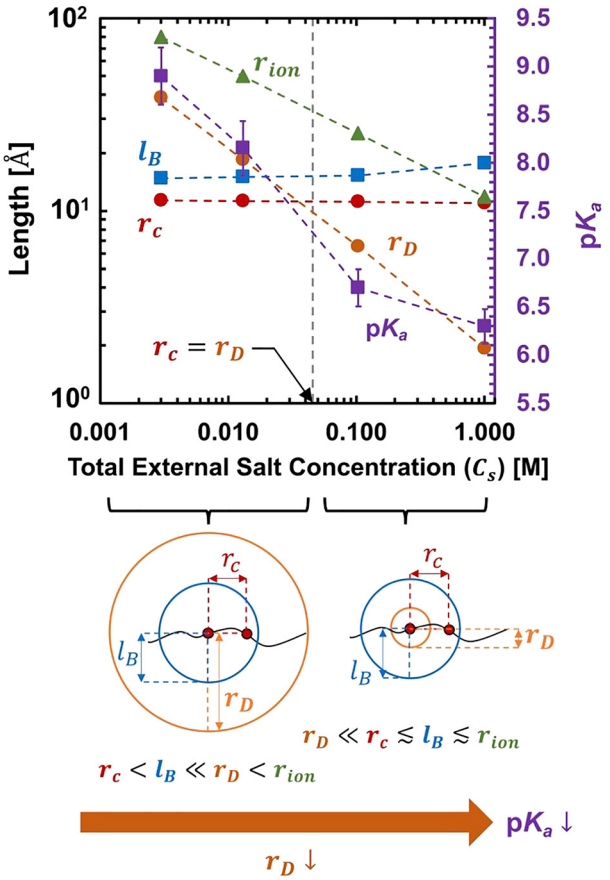


Fig. 9 Relevant length scales ($r_c$, $r_{ion}$, $l_B$, $r_D$) and p$K_a$ (*via* POT titration) *vs.* total external salt concentration ($C_s$) in different NaCl (aq) solutions.

interaction by added external salts is the dominant factor to promote dissociation and thus decrease p$K_a$. As the external salt concentration ($C_s$) increases, water swelling ($\phi_w$) in AA–PEGDA network slightly decreases due to osmotic deswelling. However, the slightly lower water swelling ($\phi_w$) has very little effect on decreasing the charged group distance in the polymer ($r_c$) and thus leads to little substantive influence on the electrostatic interaction (and, consequently, the dissociation). In our system, the screened electrostatic interaction by the added external salts is the major factor to dictate the dissociation and p$K_a$. This lowered p$K_a$ trend *via* added external salts is consistent with other theoretical and experimental dissociation reports using polyelectrolyte brushes, polymer networks and linear polymers in different salt solutions.[60,90–94]

Fig. 9 summarizes the molecular-level picture of dissociation (p$K_a$) in different external salt concentration solutions using the four relevant length scales ($r_c$, $r_{ion}$, $l_B$, and $r_D$). In lower NaCl concentration solutions (0 M $\leq C_{Nacl} \leq$ 0.01 M), the electrostatic interaction energy is dominant and maximized in dilute conditions and thus suppresses the dissociation and increases p$K_a$. The charged group distance in the polymer ($r_c$) is shorter than the Bjerrum length ($l_B$) and substantially shorter than the Debye screening length ($r_D$) ($r_c < l_B \ll r_D < r_{ion}$). The unscreened electrostatic interaction is dominant over the

thermal energy for random motion. Thus, the ions are strongly associated with the charged groups, suppressing dissociation and increasing p$K_a$. In contrast, in higher NaCl concentration solutions (0.1 M $\leq C_{Nacl} \leq$ 1.0 M), the electrostatic interaction energy is screened by the added external salts. The charged group distance in the polymer ($r_c$) and the Bjerrum length ($l_B$) are significantly longer than the Debye screening length ($r_D$) ($r_D \ll r_c \lesssim l_B \lesssim r_{ion}$). The screened electrostatic interaction no longer substantially suppresses the dissociation and thus decreases p$K_a$.

Note that we also compared the four length scales ($r_c$, $r_{ion}$, $l_B$, and $r_D$) using the dielectric constants estimated by different methods in Fig. S20 and Tables S4 and S5. As the dielectric constants *via* different methods slightly decreases, Bjerrum length ($l_B$) slightly increases and Debye screening length ($r_D$) decreases, respectively (see eqn (20) and (21)) as expected. However, regardless of the slight change in the dielectric constants, the relative order of these length scales are consistent in the external NaCl (aq) concentration range.

In addition, we compared the four length scales ($r_c$, $r_{ion}$, $l_B$, and $r_D$) assuming a point charge with those assuming a spherical ion ($r_{c,eff}$, $r_{ion,eff}$, $l_B$, and $r_D$) in Fig. S22 and Table S6 (see Section S3). $r_{c,eff}$ and $r_{ion,eff}$ (assuming a spherical ion) are moderately smaller than $r_c$ and $r_{ion}$ (assuming a point charge), respectively, but both pairs ($r_c$ and $r_{c,eff}$ as well as $r_{ion}$ and $r_{ion,eff}$) are in a similar range of order. Thus, the relative standing of these four length scales ($r_{c,eff}$, $r_{ion,eff}$, $l_B$, and $r_D$) remains the same as those assuming a point charge as shown in Fig. S22.

### 4.6. Comparison with other AA-based polymers in literature: Effect of external salt concentration ($C_s$) on dissociation

In Fig. 10, p$K_a$ data of 10-2 AA-PEGDA network in different NaCl (aq) solutions were compared with those of other acrylic acid (AA)-containing polymers in the literature. Our motivation was to construct a comprehensive understanding of dissociation process in the 10-2 network along with other similar weakly charged AA-based polymers. Toward this aim, we selected relevant AA-containing polymers including linear PAA polymers with different molecular weights ($\bar{M}_w$ = 2–450 kg mol$^{-1}$)[26] and cross-linked PAA polymers and poly(methacrylic acid) (PMA) polymers in dilute and concentrated salt solutions.[27,28] Despite the fact that their polymer form factors (*e.g.*, dissolved polymer solutions with different concentrations, porous beads with different porosities, and thin films), cross-linker types and concentrations (*e.g.*, divinylbenzene, PEGDA) and external salt conditions (*e.g.*, salt type and concentrations) of these reports are different from those of our AA–PEGDA series in this study, these polymers were chosen since their reports contain detailed information on polymer composition and dissociation data ($\alpha$ *vs.* pH) for a reasonable comparison.

Note that, compared to other AA-based polymers in the literature, our AA–PEGDA series was formed into thin films of uniform-thickness and the experiments were conducted in different NaCl (aq) solutions (0–1 M). Conversely, in the literature, linear PAA polymers were dissolved in dilute solutions (NaOH $C_s$ = 0.05–0.09 M). Cross-linked PAA and PMA polymers were formed into porous beads and titrated in dilute conditions ($C_s$ = 0.03–0.06 M). Other cross-linked PAA polymers were prepared into porous beads (20–40 mesh) and titrated in 1 M potassium chloride (KCl) (aq) solution.[26–28]

Although limitations exist for direct comparisons, Fig. 10 shows a general p$K_a$ trend *vs.* cross-linking density ($\nu_t$) of our AA–PEGDA network along with other AA-based polymers in the literature. We reported the overall trend with detailed discussions in our previous paper.[23] Generally, (1) first, compared to the p$K_a$ of AA monomer (4.24–4.60), linear PAA polymers with increasing polymer chain length ($\bar{M}_w$ = 2–450 kg mol$^{-1}$) show increased p$K_a$ range (p$K_a$ = 5.41–5.86) since covalently bonded longer chains suppress the dissociation.[23,27,28,30,39,81,82] (2) Secondly, cross-linked PAA and PMA polymers with increasing cross-linking density ($\nu_t$) show higher p$K_a$ values in both dilute and concentrated solutions. Cross-linked networks restrict chain conformation, hindering dissociation and increasing p$K_a$.[23,25,27,28,39,44,86,87] Our AA–PEGDA series

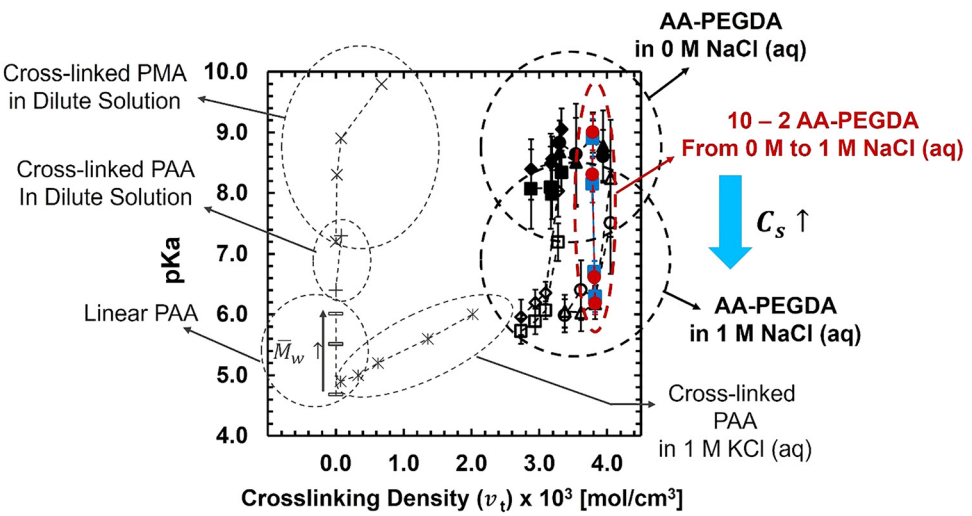


Fig. 10 Comparison with other AA-containing polymers in the literature.

(mIEC = 0–4 mequiv. per g and PEGDA cross-linker length $n$ = 10 and 13) also shows an increased p$K_a$ with increased cross-linking density ($\nu_t$) as reported previously.[23] (3) Thirdly, as external salt concentration increases, p$K_a$ decreases due to the enhanced electrostatic screening effects *via* the added external salts. Reduced electrostatic repulsion between charged groups promotes dissociation and decreases p$K_a$.[81,83,84]

Compared to other AA-based polymers in the literature, the dissociation behavior of the 10-2 network (in the fixed cross-linking density ($\nu_t$) of 3.8 mol cm$^{-3}$) is consistent with the overall trend of other AA-based polymers. Our 10-2 network shows decreasing p$K_a$ trend with increasing external salt concentration (0–1.0 M NaCl (aq)) due to the screened electrostatic interaction *via* the added external salts. To the best of our knowledge, this is the first systematic study of the dissociation process conducted using thin films of uniform thickness, with controlled variations in polymer composition and external salt concentrations. Our systematic AA–PEGDA library can help us understand the molecular picture of the dissociation in weakly charged polymers.

## 5. Conclusion

Charged polymer membranes have gained greater attention as a platform for sustainable technologies in energy, environment, and health. We previously designed a series of weak polyelectrolyte membranes, *i.e.*, cross-linked acrylic acid (AA)–poly(-ethylene glycol) diacrylate (PEGDA) (AA–PEGDA) random copolymer networks with a wide ion-exchange capacity (IEC = 0–4 mequiv. per g) range and limited water swelling. Weakly acidic, acrylic acid (AA) monomer was chosen as a charged block. Poly(ethylene glycol)diacrylates (PEGDAs) with different molecular weights were used as cross-linkers to limit water swelling. In this model polymer, we can systematically change the amount of charged groups in one fixed chemical structure without changing polymer morphology while limiting high water swelling. This system uniquely enables us to develop a systematic, mechanistic understanding of ion and water transport in charged polymer membranes.

Toward this goal, it is essential to understand the dissociation process *vs.* varied external salt conditions in the weakly charged AA–PEGDA series. Here, we reported the dissociation process in the representative chemical structure of AA–PEGDA series, *i.e.*, 10-2 AA–PEGDA network in different NaCl (aq) solutions (0 M, 0.01 M, 0.1 M and 1 M NaCl (aq)). Two analytical methods were used to rigorously measure the dissociation process in both 1) a solution phase (*via* POT titration) and 2) a polymer phase (*via* ATR–FTIR analysis). The pre-titration study confirmed that our AA–PEGDA series shows a very small dissociation degree ($\alpha$ = 0–4%) without a strong base in different NaCl (aq) solutions. Although the extent of dissociation degree ($\alpha$) is very small, the dissociation trend correlates well with the polymer composition (mIEC and $n$) and external salt concentrations. When titrated, both POT titration (detecting a solution phase) and ATR–FTIR analysis (probing a polymer phase) describe the dissociation process well and show similar ranges of dissociation parameters ($\alpha$, p$K_a$). The dissociation behavior in the 10-2 network in different NaCl (aq) solutions follows the modified Henderson–Hasselbalch equation, showing decreased p$K_a$ with increasing external salt concentrations. The overall dissociation trend was also described well by comparing four relevant molecular-level, physical length scales ($r_c$, $r_{ion}$, $l_B$, and $r_D$) in the system.

In the lower NaCl concentration solutions (0 M $\leq C_{Nacl} \leq$ 0.01 M), the relative standing of these four length scales ($r_c < l_B \ll r_D < r_{ion}$) represents that the enhanced electrostatic interaction in dilute conditions is the dominant factor to suppress the dissociation and thus increase p$K_a$. In the higher NaCl concentration solutions (0.1 M $\leq C_{Nacl} \leq$ 1.0 M), the relative order of these four length scales ($r_D \ll r_c \lesssim l_B \lesssim r_{ion}$) indicates that, the screened electrostatic interaction by added external salts is the dominant factor to promote dissociation and thus decreases p$K_a$. As the external salt concentration increases (0–1.0 M NaCl (aq)), water swelling in the AA–PEGDA network slightly decreases due to osmotic deswelling. However, the slightly lower water swelling has very little effect on effectively decreasing the charged group distance in the polymer ($r_c$), and thus, leads to little substantive influence on the electrostatic interaction (thus, the dissociation). In our system, the screened electrostatic interaction by the added external salts is the major factor to dictate the dissociation and p$K_a$. Our multiscale analysis of dissociation across varying external salt concentrations provides a pathway to tune the dissociation behavior of weakly charged polymers and achieve desired transport properties for target applications. Together, our model system can help us design innovative charged polymer membranes for sustainable technologies.

## Conflicts of interest

There is no conflicts to declare.

## Data availability

All experimental data reported in this article are included in the manuscript and the supplementary information (SI). Supplementary information: polymer composition, pre-titration and titration procedures, dielectric constants, ATR–FTIR analysis, p$K_a$ and $B$ values, and physical length scales. See DOI: https://doi.org/10.1039/d5sm01024a.

## Acknowledgements

This research is supported by the startup fund of the Department of Chemical Engineering at Pennsylvania State University and ACS Petroleum Research Fund (PRF) Doctoral New Investigator (DNI) grant (66049-DNI9). C. M. R. was supported by the Research Experience and Mentoring (PEM) Program by NSF IUCRC Center for Membrane Applications, Science and Technology (MAST) (Award Number: 1841474). K. M. T. was

 

supported by the NSF REU Biofellowship. We thank valuable discussion with Dr Ralph Colby in the Department of Materials Science and Engineering at Pennsylvania State University.

## References

1 N. Kaushika, K. Reddy and K. Kaushik, *Sustainable energy and the environment: A clean technology approach*, Springer, 2016, DOI: 10.1007/978-3-319-29446-9.
2 E. Commission, *Implementing the Water-Energy-Food-Ecosystems Nexus and Achieving the Sustainable Development Goals*, UNESCO Publishing, 2021.
3 D. Keairns, R. Darton and A. Irabien, The energy-water-food nexus, *Annu. Rev. Chem. Biomol. Eng.*, 2016, **7**(1), 239–262, DOI: 10.1146/annurev-chembioeng-080615-033539.
4 National Academies of Sciences, Engineering, and Medicine, Division on Earth and Life Studies, Board on Chemical Sciences and Technology, Committee on a Research Agenda for a New Era in Separation Science, *A Research Agenda for Transforming Separation Science*, 2019.
5 K.-V. Peinemann and S. P. Nunes, *Membranes for life sciences*, John Wiley & Sons, 2011.
6 M. Elimelech and W. A. Phillip, The future of seawater desalination: energy, technology, and the environment, *Science*, 2011, **333**(6043), 712–717, DOI: 10.1126/science.1200488.
7 A. Mauger, C. M. Julien, A. Paolella, M. Armand and K. Zaghib, Building better batteries in the solid state: A review, *Materials*, 2019, **12**(23), 3892, DOI: 10.3390/ma12233892.
8 H. Zhang and P. K. Shen, Recent development of polymer electrolyte membranes for fuel cells, *Chem. Rev.*, 2012, **112**(5), 2780–2832, DOI: 10.1021/cr200035s.
9 J. R. Werber, C. O. Osuji and M. Elimelech, Materials for next-generation desalination and water purification membranes, *Nat. Rev. Mater.*, 2016, **1**(5), 1–15, DOI: 10.1038/natrevmats.2016.18.
10 W.-Y. Zhao, M. Zhou, B. Yan, X. Sun, Y. Liu, Y. Wang, T. Xu and Y. Zhang, Waste conversion and resource recovery from wastewater by ion exchange membranes: state-of-the-art and perspective, *Ind. Eng. Chem. Res.*, 2018, **57**(18), 6025–6039, DOI: 10.1021/acs.iecr.8b00519.
11 B. D. Freeman and I. Pinnau, *Gas and liquid separations using membranes: an overview*, 2004, DOI: 10.1021/bk-2004-0876.ch001.
12 H. J. Oh, M. S. Aboian, M. Y. Yi, J. A. Maslyn, W. S. Loo, X. Jiang, D. Y. Parkinson, M. W. Wilson, T. Moore and C. R. Yee, 3D printed absorber for capturing chemotherapy drugs before they spread through the body, *ACS Cent. Sci.*, 2019, **5**(3), 419–427, DOI: 10.1021/acscentsci.8b00700.
13 H. Stapf, F. Selbmann, Y. Joseph and P. Rahimi, Membrane-based nems/mems biosensors, *ACS Appl. Electron. Mater.*, 2024, **6**(4), 2120–2133, DOI: 10.1021/acsaelm.3c01732.
14 G. Hazarika, S. V. Jadhav and P. G. Ingole, Exploring the potential of polymeric membranes in cutting-edge chemical and biomedical applications: A review, *Mater. Today Commun.*, 2024, 109022, DOI: 10.1016/j.mtcomm.2024.109022.
15 V. Siracusa, Food packaging permeability behaviour: A report, *Int. J. Polym. Sci.*, 2012, **2012**(1), 302029, DOI: 10.1155/2012/302029.
16 J. Kamcev, D. R. Paul and B. D. Freeman, Effect of fixed charge group concentration on equilibrium ion sorption in ion exchange membranes, *J. Mater. Chem. A*, 2017, **5**(9), 4638–4650, DOI: 10.1039/C6TA07954G.
17 J. Kamcev, C. M. Doherty, K. P. Lopez, A. J. Hill, D. R. Paul and B. D. Freeman, Effect of fixed charge group concentration on salt permeability and diffusion coefficients in ion exchange membranes, *J. Membr. Sci.*, 2018, **566**, 307–316, DOI: 10.1016/j.memsci.2018.08.053.
18 N. Yan, R. Sujanani, J. Kamcev, M. Galizia, E.-S. Jang, D. R. Paul and B. D. Freeman, Influence of fixed charge concentration and water uptake on ion sorption in AMPS/PEGDA membranes, *J. Membr. Sci.*, 2022, **644**, 120171, DOI: 10.1016/j.memsci.2021.120171.
19 E.-S. Jang, J. Kamcev, K. Kobayashi, N. Yan, R. Sujanani, T. J. Dilenschneider, H. B. Park, D. R. Paul and B. D. Freeman, Influence of water content on alkali metal chloride transport in cross-linked Poly (ethylene glycol)Diacrylate. 1. Ion sorption, *Polymer*, 2019, **178**, 121554, DOI: 10.1016/j.polymer.2019.121554.
20 E.-S. Jang, J. Kamcev, K. Kobayashi, N. Yan, R. Sujanani, T. J. Dilenschneider, H. B. Park, D. R. Paul and B. D. Freeman, Influence of water content on alkali metal chloride transport in cross-linked Poly (ethylene glycol)diacrylate. 2. Ion diffusion, *Polymer*, 2020, **192**, 122316, DOI: 10.1016/j.polymer.2020.122316.
21 N. Yan, R. Sujanani, J. Kamcev, E.-S. Jang, K. Kobayashi, D. R. Paul and B. D. Freeman, Salt and ion transport in a series of crosslinked AMPS/PEGDA hydrogel membranes, *J. Membr. Sci.*, 2022, **653**, 120549, DOI: 10.1016/j.memsci.2022.120549.
22 Y. Kim, T. Kim, D. E. Kang, R. B. Kracaw, A. J. Lukaszewski, J. S. Szymanski, C. M. Rahman, M. A. Shaqfeh, K. M. Tierney and H. Doan, *et al.*, Weak polyelectrolyte membranes with a wide ion-exchange capacity (IEC) range and limited water swelling in clean technologies for sustainability, *ACS Appl. Polym. Mater.*, 2024, **6**(18), 11334–11349, DOI: 10.1021/acsapm.4c01877.
23 Y. Kim, T. Kim, D. E. Kang, J. S. Szymanski, R. B. Kracaw, A. J. Lukaszewski, K. M. Tierney, M. A. Shaqfeh, C. M. Rahman and H. J. Oh, Determination of Carboxyl Dissociation Degree and pKa in Weak Polyelectrolyte Membranes via POT Titration and FTIR Analysis for Clean Technologies in Sustainability, *Macromolecules*, 2024, **57**(22), 10844–10860, DOI: 10.1021/acs.macromol.4c02139.
24 F. G. Helfferich, *Ion exchange*, Courier Corporation, 1995.
25 V. Soldatov, Potentiometric titration of ion exchangers, *React. Funct. Polym.*, 1998, **38**(2–3), 73–112, DOI: 10.1016/S1381-5148(98)00018-2.
26 M. Müller, L. Wirth and B. Urban, Determination of the carboxyl dissociation degree and pKa value of mono and

polyacid solutions by FTIR titration, *Macromol. Chem. Phys.*, 2021, **222**(4), 2000334, DOI: 10.1002/macp.202000334.

27 S. Fisher and R. Kunin, Effect of Cross-linking on the Properties of Carboxylic Polymers. I. Apparent Dissociation Constants of Acrylic and Methacrylic Acid Polymers, *J. Phys. Chem.*, 1956, **60**(8), 1030–1032, DOI: 10.1021/j150542a003.

28 H. P. Gregor, M. J. Hamilton, J. Becher and F. Bernstein, Studies on ion exchange resins. XIV. Titration, capacity and swelling of Methaerylic acid resins, *J. Phys. Chem.*, 1955, **59**(9), 874–881, DOI: 10.1021/j150531a017.

29 O. Coronell, B. J. Marinas and D. G. Cahill, Depth heterogeneity of fully aromatic polyamide active layers in reverse osmosis and nanofiltration membranes, *Environ. Sci. Technol.*, 2011, **45**(10), 4513–4520, DOI: 10.1021/es200007h.

30 T. Swift, L. Swanson, M. Geoghegan and S. Rimmer, The pH-responsive behaviour of poly (acrylic acid) in aqueous solution is dependent on molar mass, *Soft. Matter.*, 2016, **12**(9), 2542–2549, DOI: 10.1039/C5SM02693H.

31 S. Al-Amshawee, M. Y. B. M. Yunus, A. A. M. Azoddein, D. G. Hassell, I. H. Dakhil and H. A. Hasan, Electrodialysis desalination for water and wastewater: A review, *Chem. Eng. J.*, 2020, **380**, 122231, DOI: 10.1016/j.cej.2019.122231.

32 H. Zhang, W. Lu and X. Li, Progress and perspectives of flow battery technologies, *Electrochem. Energy Rev.*, 2019, **2**, 492–506, DOI: 10.1007/s41918-019-00047-1.

33 G. M. Geise, D. R. Paul and B. D. Freeman, Fundamental water and salt transport properties of polymeric materials, *Prog. Polym. Sci.*, 2014, **39**(1), 1–42, DOI: 10.1016/j.progpolymsci.2013.07.001.

34 H. Yasuda, C. Lamaze and A. Peterlin, Diffusive and hydraulic permeabilities of water in water-swollen polymer membranes, *J. Polym. Sci., Part A-2*, 1971, **9**(6), 1117–1131, DOI: 10.1002/pol.1971.160090608.

35 H. Yasuda, C. Lamaze and L. Ikenberry, Permeability of solutes through hydrated polymer membranes. Part I. Diffusion of sodium chloride, *Die Makromol. Chem.*, 1968, **118**(1), 19–35, DOI: 10.1002/macp.1968.021180102.

36 H. Yasuda, L. Ikenberry and C. Lamaze, Permeability of solutes through hydrated polymer membranes, Part II. Permeability of water soluble organic solutes, *Die Makromol. Chem.*, 1969, **125**(1), 108–118, DOI: 10.1002/macp.1969.021250111.

37 W. Xie, H. Ju, G. M. Geise, B. D. Freeman, J. I. Mardel, A. J. Hill and J. E. McGrath, Effect of free volume on water and salt transport properties in directly copolymerized disulfonated poly (arylene ether sulfone) random copolymers, *Macromolecules*, 2011, **44**(11), 4428–4438, DOI: 10.1021/ma102745s.

38 H. Ju, A. C. Sagle, B. D. Freeman, J. I. Mardel and A. J. Hill, Characterization of sodium chloride and water transport in crosslinked poly (ethylene oxide) hydrogels, *J. Membr. Sci.*, 2010, **358**(1–2), 131–141, DOI: 10.1016/j.memsci.2010.04.035.

39 Y. Kim, M. A. Shaqfeh, C. M. Rahman, R. B. Kracaw, S. D. Marotta, N. S. Kanumuru, A. Chandra, A. J. Lukaszewski, L. Collins and H. J. Oh, Carboxyl Dissociation Degree and pKa of Weak Polyelectrolyte Membranes in Dilute and Concentrated External Salt Solutions for Sustainable Technologies, *Macromolecules*, 2026, DOI: 10.1021/acs.macromol.5c02531.

40 P. J. Flory, *Principles of polymer chemistry*, Cornell university press, 1953.

41 H. Lin, T. Kai, B. D. Freeman, S. Kalakkunnath and D. S. Kalika, The effect of cross-linking on gas permeability in cross-linked poly (ethylene glycol diacrylate), *Macromolecules*, 2005, **38**(20), 8381–8393, DOI: 10.1021/ma0510136.

42 W. Stumm and J. J. Morgan, *Aquatic chemistry: chemical equilibria and rates in natural waters*, John Wiley & Sons, 2013.

43 E. Riché, A. Carrié, N. Andin and S. Mabic, High-purity water and pH, *Am. Lab.*, 2006, **38**(13), 22.

44 R. Kunin and S. Fisher, Effect of cross-linking on the properties of carboxylic polymers. II. apparent dissociation constants as a function of the exchanging monovalent cation, *J. Phys. Chem.*, 1962, **66**(11), 2275–2277, DOI: 10.1021/j100817a513.

45 D. Walsh and P. Zoller, *Standard pressure volume temperature data for polymers*, CRC press, 1995.

46 H. Lin and B. D. Freeman, Gas solubility, diffusivity and permeability in poly (ethylene oxide), *J. Membr. Sci.*, 2004, **239**(1), 105–117, DOI: 10.1016/j.memsci.2003.08.031.

47 J. Brandrup, E. H. Immergut, E. A. Grulke, A. Abe and D. R. Bloch, *Polymer handbook*, Wiley, New York, 1999.

48 H. J. Oh, J. E. McGrath and D. R. Paul, Water and salt transport properties of disulfonated poly (arylene ether sulfone) desalination membranes formed by solvent-free melt extrusion, *J. Membr. Sci.*, 2018, **546**, 234–245, DOI: 10.1016/j.memsci.2017.09.070.

49 W. Xie, J. Cook, H. B. Park, B. D. Freeman, C. H. Lee and J. E. McGrath, Fundamental salt and water transport properties in directly copolymerized disulfonated poly (arylene ether sulfone) random copolymers, *Polymer*, 2011, **52**(9), 2032–2043, DOI: 10.1016/j.polymer.2011.02.006.

50 T. J. Zimudzi, K. E. Feldman, J. F. Sturnfield, A. Roy, M. A. Hickner and C. M. Stafford, Quantifying carboxylic acid concentration in model polyamide desalination membranes via Fourier transform infrared spectroscopy, *Macromolecules*, 2018, **51**(17), 6623–6629, DOI: 10.1021/acs.macromol.8b01194.

51 G. M. Geise, L. P. Falcon, B. D. Freeman and D. R. Paul, Sodium chloride sorption in sulfonated polymers for membrane applications, *J. Membr. Sci.*, 2012, **423**, 195–208, DOI: 10.1016/j.memsci.2012.08.014.

52 D. Kitto and J. Kamcev, Manning condensation in ion exchange membranes: A review on ion partitioning and diffusion models, *J. Polym. Sci.*, 2022, **60**(21), 2929–2973, DOI: 10.1002/pol.20210810.

53 V. P. Debye, Zur theorie der electrolyte, *Phys. Z.*, 1923, 185–206.

54 N. Bjerrum, *Untersuchungen über Ionenassoziation*, AF Høst, 1926.

55 M. E. Fisher and Y. Levin, Criticality in ionic fluids: Debye-Hückel theory, Bjerrum, and beyond, *Phys. Rev. Lett.*, 1993, **71**(23), 3826, DOI: 10.1103/PhysRevLett.71.3826.

 

56 M. Costa Reis, Ion activity models: the Debye-Hückel equation and its extensions, *ChemTexts*, 2021, **7**(2), 9, DOI: 10.1007/s40828-020-00130-x.
57 G. S. Manning, Limiting laws and counterion condensation in polyelectrolyte solutions I. Colligative properties, *J. Chem. Phys.*, 1969, **51**(3), 924–933, DOI: 10.1063/1.1672157.
58 G. S. Manning, Electrostatic free energies of spheres, cylinders, and planes in counterion condensation theory with some applications, *Macromolecules*, 2007, **40**(22), 8071–8081, DOI: 10.1021/ma071457x.
59 J. Kamcev, D. R. Paul and B. D. Freeman, Ion activity coefficients in ion exchange polymers: applicability of Manning's counterion condensation theory, *Macromolecules*, 2015, **48**(21), 8011–8024, DOI: 10.1021/acs.macromol.5b01654.
60 M. Muthukumar, 50th anniversary perspective: A perspective on polyelectrolyte solutions, *Macromolecules*, 2017, **50**(24), 9528–9560, DOI: 10.1021/acs.macromol.7b01929.
61 J. Barthel, H. Krienke, W. Kunz and W. Kunz, *Physical chemistry of electrolyte solutions: modern aspects*, Springer Science & Business Media, 1998.
62 S. M. Bannon, B. M. Tremblay, A. Boudreau, N. Sreedhar, C. Morin, C. R. Leroux, P. Phan, A. Roy, M. Paul and G. M. Geise, Characterizing Hydrated Polymers via Dielectric Relaxation Spectroscopy: Connecting Relative Permittivity, State of Water, and Salt Transport Properties of Sulfonated Polysulfones, *Macromolecules*, 2025, **58**(15), 8271–8287, DOI: 10.1021/acs.macromol.5c00616.
63 P. Barber, S. Balasubramanian, Y. Anguchamy, S. Gong, A. Wibowo, H. Gao, H. J. Ploehn and H.-C. Zur Loye, Polymer composite and nanocomposite dielectric materials for pulse power energy storage, *Materials*, 2009, **2**(4), 1697–1733, DOI: 10.3390/ma2041697.
64 R. Bikky, N. Badi and A. Bensaoula, Effective medium theory of nanodielectrics for embedded energy storage capacitors, In *Proceedings of the COMSOL Conference*, Boston, MA, USA, 2010, pp. 7–10.
65 V. D. Bruggeman, Berechnung verschiedener physikalischer Konstanten von heterogenen Substanzen. I. Dielektrizitätskonstanten und Leitfähigkeiten der Mischkörper aus isotropen Substanzen, *Ann. Phys.*, 1935, **416**(7), 636–664, DOI: 10.1002/andp.19354160705.
66 A. V. Dobrynin and M. Rubinstein, Theory of polyelectrolytes in solutions and at surfaces, *Prog. Polym. Sci.*, 2005, **30**(11), 1049–1118, DOI: 10.1016/j.progpolymsci.2005.07.006.
67 N. Noda and J. Obrzut, High frequency dielectric relaxation in polymers filled with ferroelectric ceramics, In *Materials Research Society symposia proceedings*, 2002, Materials Research Society, Warrendale, Pa., 1999, vol. 698, pp. 113–120.
68 S. Kalakkunnath, D. S. Kalika, H. Lin, R. D. Raharjo and B. D. Freeman, Molecular relaxation in cross-linked poly (ethylene glycol)and poly (propylene glycol)diacrylate networks by dielectric spectroscopy, *Polymer*, 2007, **48**(2), 579–589, DOI: 10.1016/j.polymer.2006.11.046.
69 S. M. Bannon and G. M. Geise, Application of the Born Model to Describe Salt Partitioning in Hydrated Polymers, *ACS Macro Lett.*, 2024, **13**(5), 515–520, DOI: 10.1021/acsmacrolett.4c00048.
70 M. Valiskó and D. Boda, The effect of concentration-and temperature-dependent dielectric constant on the activity coefficient of NaCl electrolyte solutions, *J. Chem. Phys.*, 2014, **140**(23), DOI: 10.1063/1.4883742.
71 J. Barthel, R. Buchner and M. Münsterer, DECHEMA Chemistry Data Series. DECHEMA, *Frankfurt aM*, 1995.
72 J. Barthel, F. Schmithals and H. Behret, *Untersuchungen zur Dispersion der komplexen Dielektrizitätskonstante wäßriger und nichtwäßriger Elektrolytlösungen*, 1970, DOI: 10.1524/zpch.1970.71.1_3.115.
73 G. M. Silva, X. Liang and G. M. Kontogeorgis, How to account for the concentration dependency of relative permittivity in the Debye–Hückel and Born equations, *Fluid Phase Equilib.*, 2023, **566**, 113671, DOI: 10.1016/j.fluid.2022.113671.
74 J. Kamcev, E.-S. Jang, N. Yan, D. R. Paul and B. D. Freeman, Effect of ambient carbon dioxide on salt permeability and sorption measurements in ion-exchange membranes, *J. Membr. Sci.*, 2015, **479**, 55–66, DOI: 10.1016/j.memsci.2014.12.031.
75 H. Zhang and G. M. Geise, Modeling the water permeability and water/salt selectivity tradeoff in polymer membranes, *J. Membr. Sci.*, 2016, **520**, 790–800, DOI: 10.1016/j.memsci.2016.08.035.
76 A. V. Goncharenko and V. M. Silkin, A Century of General Lichtenecker Equation: Between Stringency and Empiricism, Accuracy and Approximability, *Materials*, 2025, **18**(24), 5562, DOI: 10.3390/ma18245562.
77 K. Lichtenecker, Die dielektrizitatskonstante naturlicher und kunstlicher mischkorper, *Phys. Z.*, 1926, **27**, 115–158.
78 K. Chang, H. Luo and G. M. Geise, Influence of salt concentration on hydrated polymer relative permittivity and state of water properties, *Macromolecules*, 2021, **54**(2), 637–646, DOI: 10.1021/acs.macromol.0c02188.
79 K. W. Wagner, Erklärung der dielektrischen nachwirkungsvorgänge auf grund maxwellscher vorstellungen, *Arch. Elektrotech.*, 1914, **2**(9), 371–387, DOI: 10.1007/BF01657322.
80 J. Lou, T. A. Hatton and P. E. Laibinis, Effective dielectric properties of solvent mixtures at microwave frequencies, *J. Phys. Chem. A*, 1997, **101**(29), 5262–5268, DOI: 10.1021/jp970731u.
81 H. Kodama, T. Miyajima, M. Mori, M. Takahashi, H. Nishimura and S. Ishiguro, A unified analytical treatment of the acid-dissociation equilibria of weakly acidic linear polyelectrolytes and the conjugate acids of weakly basic linear polyelectrolytes, *Colloid Polym. Sci.*, 1997, **275**, 938–945, DOI: 10.1007/s003960050169.
82 T. Miyajima, M. Mori and S.-I. Ishiguro, Analysis of complexation equilibria of polyacrylic acid by a Donnan-based concept, *J. Colloid Interface Sci.*, 1997, **187**(1), 259–266, DOI: 10.1006/jcis.1996.4694.
83 S. Lifson and A. Katchalsky, The electrostatic free energy of polyelectrolyte solutions. II. Fully stretched macromolecules, *J. Polym. Sci.*, 1954, **13**(68), 43–55, DOI: 10.1002/pol.1954.120136804.

84 I. Michaeli and A. Katchalsky, Potentiometric titration of polyelectrolyte gels, *J. Polym. Sci.*, 1957, **23**(104), 683–696, DOI: 10.1002/pol.1957.1202310412.
85 N. Yan, D. R. Paul and B. D. Freeman, Water and ion sorption in a series of cross-linked AMPS/PEGDA hydrogel membranes, *Polymer*, 2018, **146**, 196–208, DOI: 10.1016/j.polymer.2018.05.021.
86 V. S. Soldatov, Quantitative presentation of potentiometric titration curves of ion exchangers, *Ind. Eng. Chem. Res.*, 1995, **34**(8), 2605–2611, DOI: 10.1021/ie00047a008.
87 H. Strobel and R. Gable, Titration studies as a means of characterizing anion-exchange resins, *J. Am. Chem. Soc.*, 1954, **76**(23), 5911–5915, DOI: 10.1021/ja01652a005.
88 T. Canal and N. A. Peppas, Correlation between mesh size and equilibrium degree of swelling of polymeric networks, *J. Biomed. Mater. Res.*, 1989, **23**(10), 1183–1193, DOI: 10.1002/jbm.820231007.
89 B. Vondrasek, C. Wen, S. Cheng, J. S. Riffle and J. J. Lesko, Hydration, ion distribution, and ionic network formation in sulfonated poly (arylene ether sulfones), *Macromolecules*, 2020, **54**(1), 302–315, DOI: 10.1021/acs.macromol.0c01855.
90 C. Balzer and Z.-G. Wang, Electroresponse of weak polyelectrolyte brushes, *Eur. Phys. J. E*, 2023, **46**(9), 82, DOI: 10.1140/epje/s10189-023-00341-3.
91 G. Ferrand-Drake del Castillo, R. L. Hailes and A. Dahlin, Large changes in protonation of weak polyelectrolyte brushes with salt concentration—Implications for protein immobilization, *J. Phys. Chem. Lett.*, 2020, **11**(13), 5212–5218, DOI: 10.1021/acs.jpclett.0c01289.
92 N. A. Kumar and C. Seidel, Polyelectrolyte brushes with added salt, *Macromolecules*, 2005, **38**(22), 9341–9350, DOI: 10.1021/ma0515735.
93 R. Arnold, The titration of polymeric acids, *J. Colloid Sci.*, 1957, **12**(6), 549–556, DOI: 10.1016/0095-8522(57)90060-0.
94 G. S. Longo, M. Olvera de La Cruz and I. Szleifer, Molecular theory of weak polyelectrolyte gels: the role of pH and salt concentration, *Macromolecules*, 2011, **44**(1), 147–158, DOI: 10.1021/ma102312y.

 